Poster sessions

Objekttyp: **Group**

Zeitschrift: **IABSE reports = Rapports AIPC = IVBH Berichte**

Band (Jahr): **52 (1986)**

PDF erstellt am: **15.05.2024**

Nutzungsbedingungen

Die ETH-Bibliothek ist Anbieterin der digitalisierten Zeitschriften. Sie besitzt keine Urheberrechte an den Inhalten der Zeitschriften. Die Rechte liegen in der Regel bei den Herausgebern.
Die auf der Plattform e-periodica veröffentlichten Dokumente stehen für nicht-kommerzielle Zwecke in Lehre und Forschung sowie für die private Nutzung frei zur Verfügung. Einzelne Dateien oder Ausdrucke aus diesem Angebot können zusammen mit diesen Nutzungsbedingungen und den korrekten Herkunftsbezeichnungen weitergegeben werden.
Das Veröffentlichen von Bildern in Print- und Online-Publikationen ist nur mit vorheriger Genehmigung der Rechteinhaber erlaubt. Die systematische Speicherung von Teilen des elektronischen Angebots auf anderen Servern bedarf ebenfalls des schriftlichen Einverständnisses der Rechteinhaber.

Haftungsausschluss

Alle Angaben erfolgen ohne Gewähr für Vollständigkeit oder Richtigkeit. Es wird keine Haftung übernommen für Schäden durch die Verwendung von Informationen aus diesem Online-Angebot oder durch das Fehlen von Informationen. Dies gilt auch für Inhalte Dritter, die über dieses Angebot zugänglich sind.

Ein Dienst der *ETH-Bibliothek*
ETH Zürich, Rämistrasse 101, 8092 Zürich, Schweiz, www.library.ethz.ch

http://www.e-periodica.ch

POSTER SESSIONS

1. Assessment of Existing Structures
2. Honshu-Shikoku Bridge Project
3. Technical Solutions

TSING YI SOUTH BRIDGE ASSESSMENT

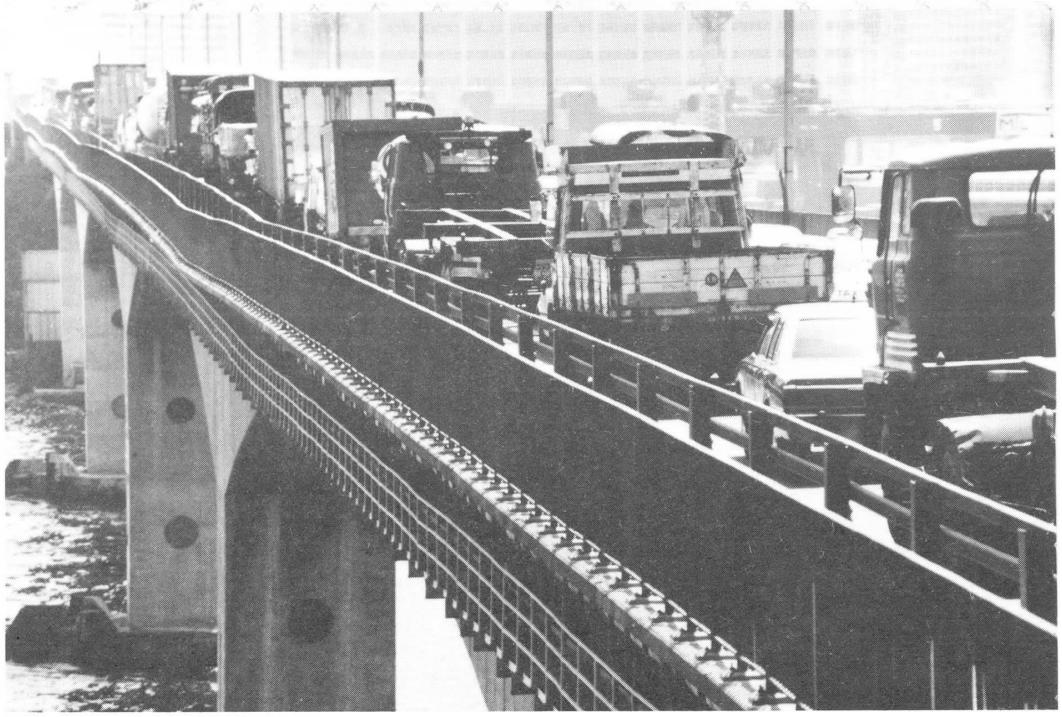

Tsing Yi South Bridge Assessment

A.S. BEARD
Associate
Mott, Hay & Anderson Far East
Hong Kong

H.S.S. TUNG
Chief Highway Engineer/Structures
Highways Department
Hong Kong

Opened to traffic in 1974, Tsing Yi South Bridge currently provides the only means of access from the mainland to the island of Tsing Yi. It was constructed by a private consortium, principally to provide access to a power station and to carry six 132 kV circuits from it to Kowloon, and upon completion was handed over to Government to operate. Since the bridge was completed, extensive development has occurred on the island, including a rapidly expanding new town. The bridge, which was built by the balanced cantilever method, is made up of five structurally independent prestressed concrete 'T' units, resulting in four main spans of 122 metres and two side spans of 61 metres, see Figure 1.

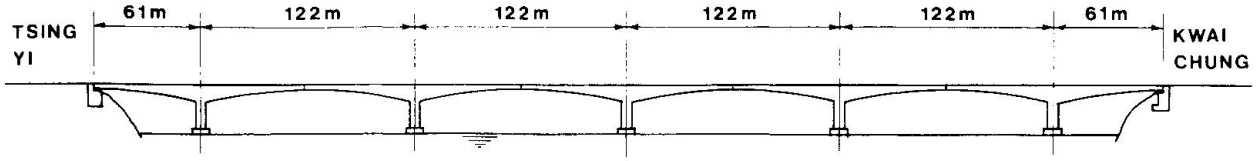

ELEVATION

Figure 1

When the expansion joints between cantilevers were replaced in 1981, it was found that the tips had deflected by nearly 200mm from their original positions and that these deflections were continuing. The deflections can be clearly seen in the poster. Concern was expressed about the service life of the bridge; this was hightened by the relatively few available construction records, together with presence within the superstructure box of the 132Kv electricity circuits. A programme of regular levelling was therefore instituted and in 1983 a thorough assessment of the structure was commissioned.

At the outset of the assessment a visual inspection was undertaken of all accessible areas of the bridge. This included removal of sections of the surfacing to examine the top flange together with underwater inspection of the piers. Simultaneously all available construction and design records were collected and personnel concerned with its construction contacted.

The visual inspection did not reveal any signs of deterioration and the available records suggested that all units were of a common design and had been constructed in a similar manner. In order to formulate a view on the condition of the bridge as quickly as possible it was therefore decided to concentrate the initial assessment on two adjacent cantilevers.

Bamboo scaffolding was erected inside the chosen cantilevers to allow a more detailed visual inspection of the top flange and to facilitate other inspection activities. Cores were extracted from the webs and top flange and tested to establish compressive strength, 'E' values and the chemical composition of the concrete. The parameters derived from these cores were used in the analysis. The chemical tests did not indicate the presence of any potentially harmful substances.

Next, vibrating wire strain gauges were attached to the concrete surface at three cross-sections on each of the two cantilevers and a series of load tests were carried out. In these tests four fully laden bulk cement carriers were parked on the deck in various patterns and readings of the strain gauges were taken. The deck was also levelled. Upon removal of each test loading the superstructure quickly rebounded to its original level. The results of analyses of the bridge under the various loading patterns agreed well with the test readings, and it was concluded that the bridge was behaving elastically. Typical results are shown in Figure 2.

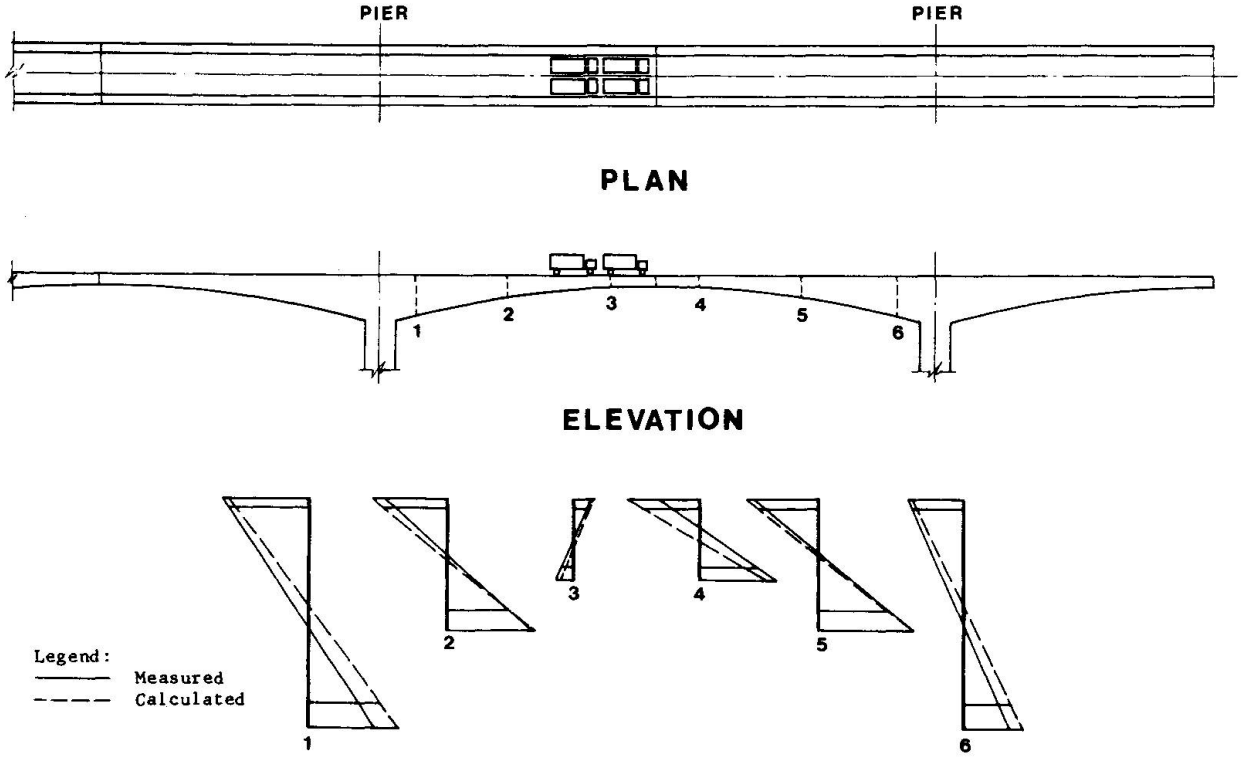

Figure 2

Traffic counts and strain gauge readings were checked against elastic analysis to determine the approximate live loading on the structure. Published annual traffic counts were then used to deduce the rate of increase in loading since the opening of the bridge.

In order to establish that all the design prestressing tendons were present, and also to check on their condition a radiograhic inspection was carried out using a Cobalt 60, 30 currie source. Radiographic plates were taken at sections across the top flange at five metre centres. However, where necessary additional plates were taken at intermediate locations. From this inspection it was concluded that all the design prestressing tendons were present but that approximately ten per cent were either partially or completely ungrouted. No signs of deterioration of either tendons or ducts were detected. A section of a typical plate showing grouted and ungrouted ducts is shown in Figure 3.

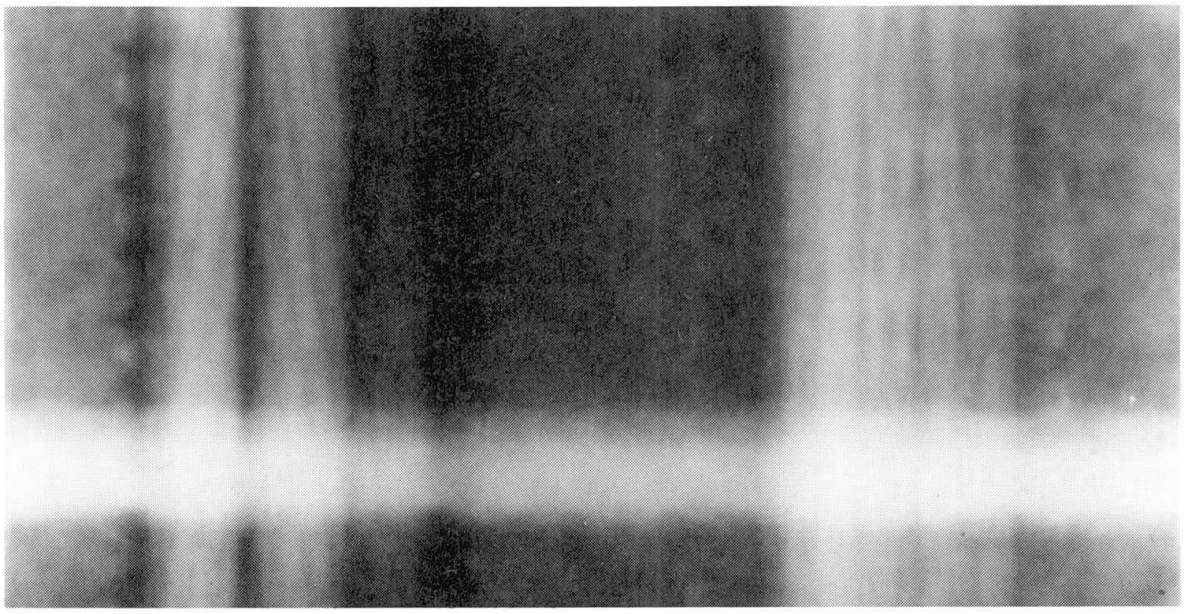

Figure 3

Throughout the period of assessement the bridge was monitored to ensure that no unexpected or sudden deterioration occurred. This monitoring continued for approximately two years and was held once a month over a twenty-four hour period. At regular intervals during the sessions the superstructure was levelled; the strain gauges read; temperature readings taken of the concrete surface, the high-voltage electricity cables and the surrounding air; and details obtained of the power loading through the cables.

Concurrent with the inspection, analysis of the bridge was carried out in two phases. The first phase covered the construction of the bridge, and the second its long-term behaviour. Level measurements had been taken of the piers and the tips of the cantilevers on 28th November 1974, about one year after structural completion. These measured values were adopted as a check on the first phase of analysis, and as the datum for long term calculations. The calculated levels for the cantilever tips on 28th November 1974 agreed very closely with those measured.

The long-term analysis, which was extended to cover a period of 125 years, investigated the effects of time-dependent loading and losses on the bridge's behaviour. These effects included the build up of live loading, variations in temperature, temperature distributions though the superstructure, concrete creep and shrinkage, and prestressing relaxation. The calculated and measured values in December 1983 were found to be in good agreement, and the calculations indicated that deflections could be expected to increase.

From the assessment it was concluded that:

(i) the bridge was generally constructed in accordance with the design;

(ii) while the servicability life of the bridge had almost been reached, the ultimate strength of the bridge was satisfactory; and,

(iii) the long-term analysis showed that the deflections, and their continuation ten years after completion could be predicted.

Subsequently inspections were extended to the remainder of the bridge and a rehabilitation scheme developed.

By
Guanglong Zhou,
Professor,
Hunan University,
Changsha, Hunan,
P.R.C.

Contributions:
Appraised & Proved by
Ministry of Machine
Building of China &
Hunan Construction Commission
Also Accepted by ASCE.

DYNAMIC DETECTIONS OF THE QULITY OF PILES

I. VERTICAL DETECTIONS

1. Determination of the Bearing Capacity of Fricton Piles:

$$P_a = \frac{0.03 f_v^2 (1+e) W_0 \sqrt{H} K_v}{K V_0}$$

2. PROGRAM: Available for Plotting SuperPosed Stress Diagrams of the Cap Beams on Piles with Stochastic Variability.

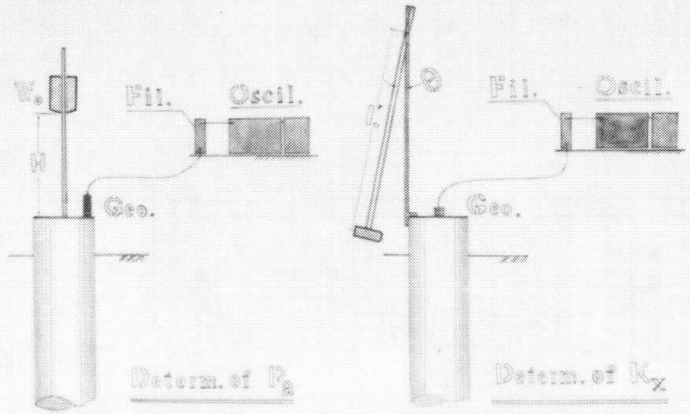

II. HORIZONTAL DETECTIONS

1. Determination of 16 Parameters—— Functions of K_x & β:

$$K_x = 25.29 \frac{f_x^2 W_e (1+e) L'\Theta}{V_0 T} K_h ; \quad \beta = \sqrt[4]{\frac{K_x}{3IEI}}$$

2. Detection of the Cracks on the Upper Portion of Piles

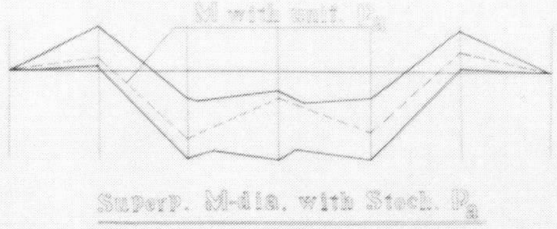

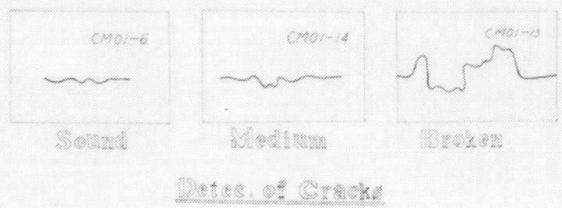

III. PRACTICE: Over 3000 Piles

IV. ECONOMY: Save Both Cost & Time 99%

V. LICENCE: No. XC—0010

Dynamic Detections of the Quality of Piles

Guanglong ZHOU
Professor
Hunan University
Changsha, Hunan, China

SUMMARY

The aim of this paper is to present an economical,time-saving and nondestructive dynamic method to replace the conventional static loading test for the detections of the bearing capacity and the quality of piles. On this basis,a method for evaluating the stress distributions in the cap-beam on piles is recommended. This can be of service to the construction analysis,decision making and implementation of the quality assurance in practice.

1. VERTICAL DETECTIONS

1.1 Determination of the Bearing Capacity of Friction Piles

The basic procedure for evaluating the bearing capacity of a friction pile is to measure the vertical frequency f_v and/or the velocity v_o of the pile excited by a vertical impact. Substituting f_v and/or v_o into the following formulae [1],[2],we can get the bearing capacity P_a of the pile:

$$P_a = \frac{0.06687\ (\ Q_1 + Q_2\ )\ (f_v)^2}{K \cdot g}$$

or

$$P_a = \frac{0.03\ f_v^2\ (\ 1 + e\ )\ W_o \sqrt{H}\ K_v}{K \cdot v_o}$$

By the latter,the information of soil and pile is unnecessary in the calculation. This method has stood a number of comparison tests and more than three thousand trials in practice.

1.2 Stresses in the Cap-beam on Piles

By the use of static testing,the influence of the variability of the behavior among piles on the stress distributions in the cap-beams is very hard to inspect. We know more or less the why,and endevour to know the how,but published articles on this problem were very scarce [3]. This uncertainty causes the waste of money by unduly raising the factor of safety. Until 1977,Dr. A. Evangelista et al presented some experimental evidence about the influence of the variability of piles on the design of cap-beam [4]. According to these data,statistic analysis showed that the scattering of stresses was found to be rather significant. The value of this pioneering contribution should be highly appreciated. It revealed quantitatively the influence in that case. However,the principal method used by them in determining the bearing capacity

of piles was the static loading test. This will prevent us from simulating their research in engineering practice,on account of the cost and the time consumed in the test,in addition to the possible damage to the piles.
On the basis of dynamic testing of piles,the calculation of the practical stresses in the cap-beams can be carried out as follows: The compliance of the pile Y_{kk} may be resonably expressed as

$$Y_{kk} = \frac{1}{10P_a}$$

The deflection coefficient V_{ki} of the cap-beam is

$$V_{ki} = \frac{c^3}{6EI} \left(\frac{S_k}{c} \right)^2 \left(\frac{3S_i}{c} - \frac{S_k}{c} \right)$$

Y_{kk} in combination with V_{ki} froms the displacement coefficient δ_{ki}:

$$\delta_{ki} = V_{ki} \text{ , and } \delta_{kk} = Y_{kk} + V_{kk}$$

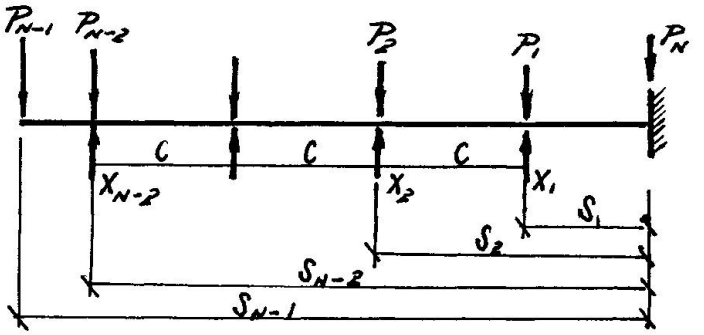

Fig. 1 The sketch of a pile-foundation

A pile-foundation shown in Fig. 1 can be properly simulated by a Winkle-type model. The corresponding simultaneous equations in the contracted form can be written as

$$\begin{cases} X_1 \delta_{k,1} - X_2 \delta_{k,2} - \cdots - X_{N-2} \delta_{k,N-2} - S_k \varphi_o - \Delta_{kP} - Y_o = 0 \\ \qquad (k = 1,2,\ldots N-2) \\ \sum_{1}^{N-2} X_i - \sum_{1}^{N} P_i = 0 \\ \sum_{1}^{N-2} X_i S_i - \sum_{1}^{N-1} M_P = 0 \end{cases}$$

This can be solved by a personal computer. There is a program available. The output is the axial forces (X_i),bending moments (M_i),shearing forces (Q_i) and settlements (Y_i) at pile heads as well as their diagrams. It is quite possible to perform the dynamic testing to determine the bearing capacities P_a of all the piles under the cap-beam. However,if only some of the representative piles have been tested,these experimental data can be dealt with by least square. By means of random number generator of a

computer, 100 or more random distributions of possible compliance of the piles can be generated. The corresponding superposed stress diagrams of the cap-beams can be drawn consecutively by the computer to show the possible extent of the influence due to the variability of the behavior of the piles,as illustrated in the Poster. The author has made use of these diagrams in designing work in lieu of conventional approximate calculations. Both economy and safety are secured.

2. HORIZONTAL DETECTIONS

2.1 Determination of Horizontal Parameters of Piles

By means of horizontal dynamic testing, 16 parameters of a pile can be determined with K_x and β,which are in terms of measured horizontal frequency f_x [1], [2]:

$$K_x = 25.29 \frac{f_x^2 W_e (1 + e) L' \theta}{v_o T} K_h ;$$

$$\beta = \sqrt[4]{\frac{K_x}{3 l EI}}$$

2.2 Detection of Cracks

The cracks in the upper portion of a pile can also be detected by the dynamic method. Soon after a horizontal impact is applied to the pile head,a waveform will be recorded by the oscilloscope in the form of one of the three categories (cf. the Poster). According to the shape,amplitude,frequency and the time-decaying of the waveform,we can predict the presence and the extent of the cracks. Among thousands of engineering piles detected by this method,more than two hundred piles were unearthed to check the reliability of the criteria. The accuracy was found to be 95%. So, this method enjoys wide support in China.

3. ACKNOWLEDGEMENTS

This research project was carried out through 1972-1985,assigned, supported,and appraised by the Ministry of Machine Building of China and Hunan Construction Commission (Licence No. XC-0010). The contribution [2] was also accepted by ASCE International Convention & Exposition,New York,N.Y.,1981.

REFERENCES

1. ZHOU GUANGLONG, Dynamic Method for Determination of Various Parameters of Piles. Selected Papers of CSCE 3rd National Conference on Soil Mechanics and Foundation Engineering.Building Engineering Press of China,1981,pp.324-330.

2. ZHOU GUANGLONG, A New Method for Dynamic Pile Testing, Preprint 81-096 of ASCE International Convention & Exposition, New York,N.Y.,1981.

3. WITAKER T., The Design of Piled Foundations.2nd edition,Pergamon Press,London,1976,p.113.

4. A. EVENGELISTA, A. PELLEGRINO & C. VIGGIANI, Variability among Piles of the Same Foundation.Proceedings of the Ninth International Conference on Soil Mechanics and Foundation Engineering, 1977,p.493.

Technische Universität Berlin
DEPARTMENT OF CIVIL ENGINEERING
CHAIR OF REINFORCED CONCRETE
Authors:
Prof. Dr.-Ing. M. Specht
Dipl.-Ing. E. Kollin
The owner of the buildings, which had been analysed, is the GEHAG Berlin

Method for assessment of working life of exterior concrete components

Surface components of existing structures are exposed to strong atmospherical deterioration. This accelerates the process of altern. It is important to decelerate this process in such a way, that our modern concrete buildings can be called durable in human time conceptions. The life expectation of these components can be extended by supplementary coating. The engineer is interested to find the latest acceptable time to coat the surface in order to reach exactly the aspired working life.

Method with weighted carbonation coefficients

In general the working life of concrete can be determined with:

$$x_k = \sqrt{2 D t} \quad (1)$$

x_k ... depth of carbonation [mm]
t ... inspection period since completion of construction [a]
D ... coefficient of carbonation [mm²/a]
The theoretical end of alkaline protection is: $t_E = \frac{c^2}{2D}$
c ... concrete cover [mm]

Tests have been carried out in 1985 within Berlin on existing structures.

Besides the age of the building we received the following data:

a) depth of carbonation: max. value, mean value, mean value of peaks
b) concrete cover: min.- and mean value.

Additionally we took into consideration a measuring error of ±1mm and a tolerance v, equivalent the increase of carbonation of the past 5 years. The results of all value combinations give different dates of working life. For the determination of a safe value the measurement data have to be weighted.
With that we obtain 4 dates for the probable appearance of the first systematic damages:

1 - earliest date without tolerance (safe value)
2 - standard date without tolerance
3 - earliest date with tolerance (prevention date)
4 - standard date with tolerance

A surface treatment should be considered at the prevention date.

Prognosis - equation (latest date for coating)

The basis is equation (1) for uncoated concrete. After coating the function between x_k and t is approximately reflected as a straight line. Including some simplifications, the derivation leads to the following equation:

$$t_A = 0{,}3 \cdot \frac{c^2}{D} + 1{,}5 \cdot \frac{c}{\sqrt{D}} - 5$$

c ... c_{MEAN}
D ... calculated with $x_{k\,MEAN-PEAK}$
t_A ... time [a] between uplift and the latest date for coating, if the working life of 100 years is to be achieved.

t_A corresponds to the prevention date.

Both of these methods of prognosis have been tested at approximately 50 existing structures within Berlin and ended up with satisfactory results. Today they are used as decisive factor for planning of finances for building maintenance. First of all, both methods are applied to central european proportions only. In future it is certainly interesting to test their quality at other locations.

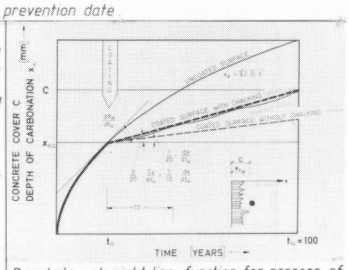

Parabola - straight line - function for process of carbonation of a concrete surface coated at t_A

Method for Serviceable Assessment of Working Life of Exterior Reinforced Concrete Components

Manfred SPECHT
Prof. Dr.-Ing.
Technische Universität Berlin
Berlin

Eckhard KALLIN
Dipl.-Ing.
Technische Universität Berlin
Berlin

Method of weighted coefficients of carbonation

As the surface has to be maintained, the number of drilling-samples can not be sufficient to get statistically safe values.

Therefore, the measurement data are weighted to obtain a usable prediction as help for decision. The basic idea is a reflection of probability and of followup damages.

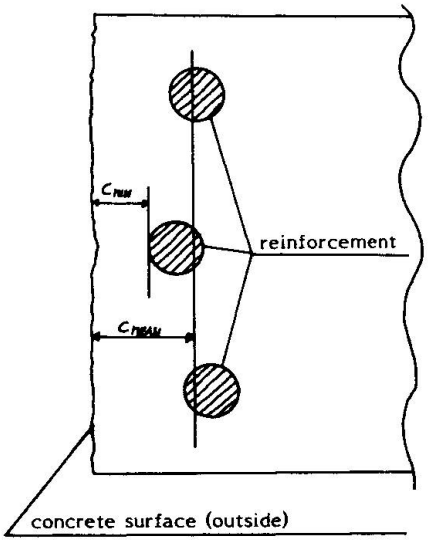

minimum and mean concrete cover

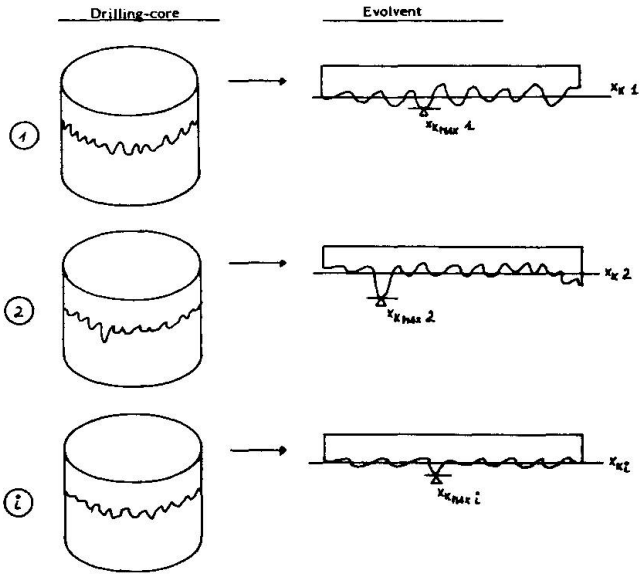

mean value	$x_{K\,mean} = \frac{\Sigma(x_{K1} + x_{K2} + \ldots + x_{Ki})}{n}$
mean value of peaks	$x_{K\,mean\text{-}peak} = \frac{\Sigma(x_{K\,max\,1} + x_{K\,max\,2} + \ldots + x_{K\,max\,i})}{n}$
maximum value	$x_{K\,max} = x_{K\,max\,2}$

combination	remarks	weighting
c_{mean} with x_{Kmean}	this combination is unreliable because it is afflicted with a large error. Damages are too severe for a promising restoration.	1/7
c_{mean} with $x_{Kmean\text{-}peak}$	Most damages arise when the front line of carbonation with its peaks meet the reinforcing steel. This combination is rather probable.	5/7
c_{min} with x_{Kmax}	This case certainly leads to the first damage but is not likely. Its appearance brings only locally restricted damage.	1/7

These factors produce four numbers of years for the likely appearance of the first systematic damages:

1) earliest date without tolerance (safe value)
2) standard date without tolerance
3) earliest date with tolerance (date of prevention)
4) standard date with tolerance

The earliest dates consider total reduction of error; the standard dates are calculated without reduction of error. The expression "systematic damages" means that in case unfavourable circumstances meet, little damages may show up locally restricted at single places. This remaining uncertainty can be accepted. Is the earliest date without tolerance far in future, for example about 100 years after construction the facade may supposed to be durable. Otherwise surface treatment should be considered not later than the earliest date with tolerance.

Method to determine a latest date for surface coating (prognosis-equation)

Today a facade coating ought to be renewed every 10 years. Lowest costs are achieved by coating at the possible latest date before the appearance of systematic damages (earliest date with tolerance).

Within the derivation of the prognosis equation we proceeded from a desired service life without damages of 100 years.

The function between depth of carbonation and coated concrete is approximated by a straight line with the gradient: $\frac{dx}{dt}(\text{straight line}) = \frac{1}{10}\frac{dx}{dt}$

For uncoated concrete the gradient at time t_A can be obtained with the function $x = \sqrt{2 \cdot D \cdot t}$:

$$\frac{dx}{dt} = \sqrt{\frac{2D}{t_A}} \cdot \frac{1}{2} \quad ; \quad t_A \neq 0 \quad \curvearrowright \quad \frac{dx}{dt} = \frac{1}{20} \cdot \sqrt{\frac{2D}{t_A}}$$

statement: $c = x_A + \frac{dx}{dt}(t_N - t_A)$ with $x_A = \sqrt{2 \cdot D \cdot t_A}$ and $t_N = 100$ years

$$\curvearrowright \quad c = \sqrt{2 \cdot D \cdot t_A} + \frac{1}{20} \cdot \sqrt{\frac{2 \cdot D}{t_A}} \quad (100 - t_A)$$

After some transformations this leads to the following equation:

$$t_A = \frac{c^2}{3{,}6 \cdot D} - 5{,}3 + 1{,}7 \frac{c}{\sqrt{D}} \sqrt{\frac{c^2}{39D} - 1}$$

With the results measured in Berlin the statistic interpretation of the term $\sqrt{\frac{c^2}{39D} - 1}$ of equation (5) in consideration of c_{mean} with $D_{mean\text{-}peak}$ as also with D_{max} leads to the factor 0,9 at an average. Therefore the last term of equation (5) comes to:

$$1{,}7 \frac{c}{\sqrt{D}} \cdot 0{,}9 \approx 1{,}5 \cdot \frac{c}{\sqrt{D}}$$

Including these simplifications and specialities of the previous listed results, the approximation ends in:

$$t_A = 0{,}3 \frac{c^2}{D} + 1{,}5 \cdot \frac{c}{\sqrt{D}} - 5$$

FATIGUE DAMAGE AND REPAIR OF STEEL RAILWAY BRIDGES IN JAPAN

H. Abe : Univ. of Utsunomiya
K. Sakamoto ; Japan National Railways
M. Abe ;

Fatigue damages have been occasionally experienced in structural details of railway bridges, because relatively large train loading is repeated in many cycles. Fig. 1 shows a schematic of the through type steel railway bridge and locations of fatigue cracks, as an example.

(A) COPED CROSS BEAM

Failure Mode : A crack is originated at the cope corner or the toe of fillet weld at the cope formed for connection with the main girder. It develops diagonally in the web plate, as shown in Fig. 2. It occurs even in case the lower flange of the main girder and that of the cross beam are connected with each other.

Cause : Both insufficiency of resisting moment of the beam due to the coping and local stress concentration are the causes of crack.

Repair : The web plate of the cross beam is locally reinforced by bolting additional plates, as shown in Fig. 3.

(B) COPED STRINGER

Failure Mode : A crack develops at the cope corner of stringer web, where the lower flange is cut short for connection with the cross beam, as shown in Fig. 4.

Cause : The lower flange of a stringer tends to be displaced sideways during train passage and a stress concentration takes place at the cope corner.

Repair : In case the crack is small, the lower flange is connected with the web, as shown in Fig. 5. But in case the damage is significant, the whole stringer is replaced by a new one.

(C) WEB PLATE NEAR VERTICAL STIFFENER END

Failure Mode : A crack develops in the web plate at the toe of fillet weld around the lower scalloped end of an intermediate stiffener, as shown in Fig. 6.

Cause : In addition to the in-plane-deformation due to the bending moment, the out-of-plane deformation due to vibration of the web plate or due to relative lateral displacement between the web and the lower flange causes this kind of crack.

Repair : Local reinforcing plates are bolted, as shown in Fig. 7.

Fig. 1

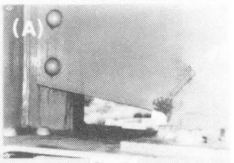

Fig. 2.

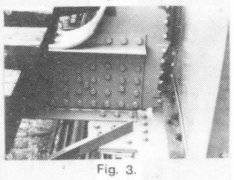

Fig. 3.

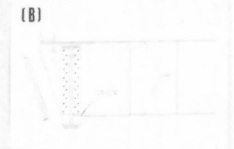

Fig. 4.

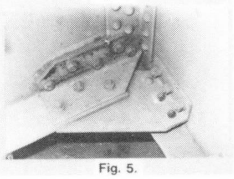

Fig. 5.

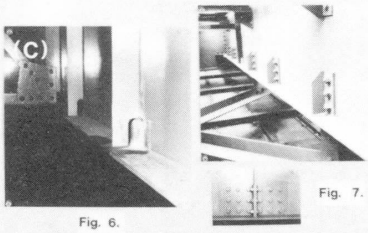

Fig. 6.

Fig. 7.

Fatigue Damage and Repair of Steel Railway Bridges in Japan

Hidehiko ABE
Professor
University of Utsunomiya
Tokyo, Japan

Kenji SAKAMOTO
Senior Engineer
Structure Design Office, JNR
Tokyo, Japan

Makoto ABE
Design Engineer
Structure Design Office, JNR
Tokyo, Japan

1. Introduction

In general, railway bridges are actually subjected to repeated train loading of a magnitude comparable to that assumed in design. In result, some inadequately designed or manufactured structural details have suffered fatigue cracks. In this poster three representative types of fatigue damages shown in Fig. 1 in Poster are dealt with.

2. Cope of Floor Beam Web

As seen in Fig. 2 in Poster, a crack initiated from the cope at the lower corner of floor beam of a through girder bridge. Such cracks have occurred in a few end floor beams and one intermediate floor beam. Their lower flanges were connected by gusset plates with those of the main girders. Fig. I shows an example of the stress variation during passage of a train in the vicinity of the cope. Then, half-scale models, in which the horizontal lengths

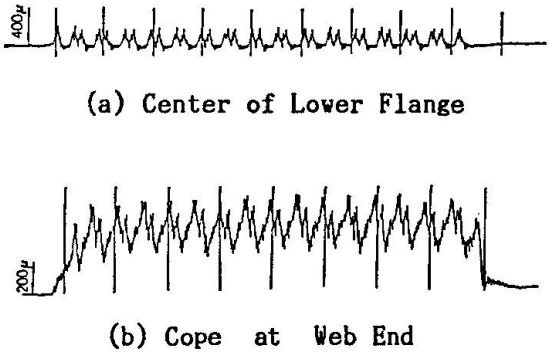

Fig.I Observed Stress Variations at End Floor Beam

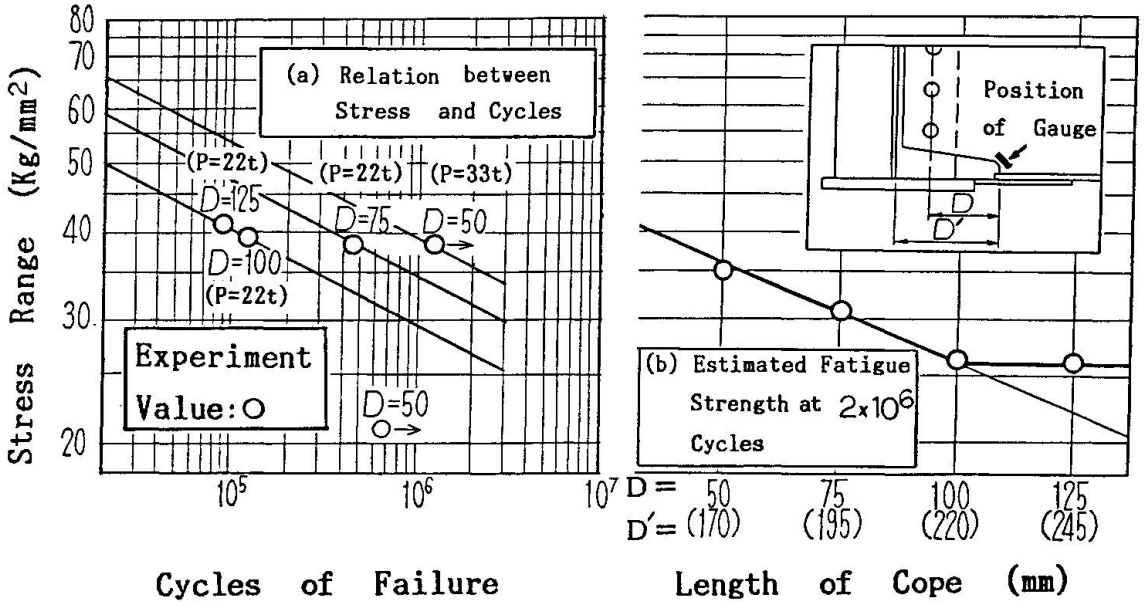

Fig. II Fatigue Strength of Coped Portion of Floor Beam

of the copes were varied, were tested under repeated loading and developed the same kind of crack as seen in the actual bridges. Both the FEM analysis and the model test revealed that the local tensile stress along the periphery of the cope became greater and consequently the fatigue strength decreased, as the cope length increased, as shown in Fig. II .

In the damaged floor beams holes were drilled at the tips of fatigue cracks in order to releave the stress and steel plates were attached by high-strength-bolts , as shown in Fig. 3 in Poster. The details of currently designed bridges have been improved as illustrated in Fig. III. The whole width of at least a half width of the lower flange of floor beam is extended to its end.

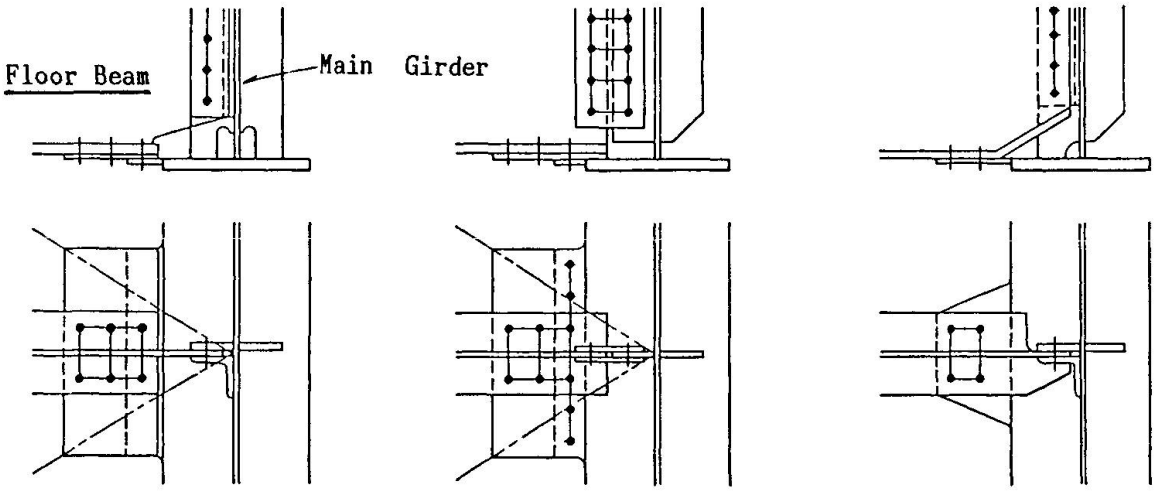

(a) Defective Details (b) Examples of Improved Details

Fig. III Details of Floor Beam

3. Cope of Stringer Web

In a stringer where the lower flange was cut short as shown in Fig. IV (a), and only the web plate was connected with the web of floor beam, a crack started from the cope , as shown in Fig. 4 in Poster. According to the observation of an actual bridge, the coped part was subjected to a high local tensile stress, because of the loss of flanges and, moreover, the lower flange moved sideways by a small amount. It is supposed, then, that the combined effect developed a crack from the cope.

In case the damage was signifficant, a small hole was drilled at the tip of the crack and the lower flange was fixed to the web of floor beam, as shown in Fig. 5 in Poster and, if necessary, additional plates were attached to the end portion of the web. In case the lower flanges of adjacent stringers are connected with each other, or a half width of the lower flange is extended to the end of the web, as shown in Fig. IV (b), there has been no instance of this kind of crack.

4. Crack in Web at Scallop of Vertical Stiffener of Web Plate

An intermediate vertical stiffener is provided with a scallop-cut at its upper and lower ends, in order to allow the longitudinal weld between the flange and the web to pass continuously and the lower end of the stiffener is not welded usually, so that fatigue strength of the lower flange may not be reduced. For the same purpose, a rather high scallop is

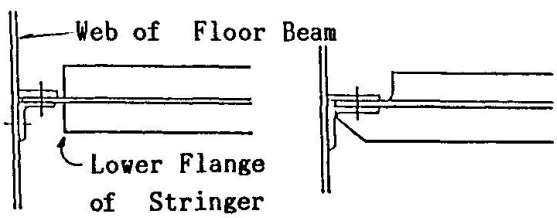

(a) Crack occurred (b) No crack occurred

Fig. IV Details of Stringer

often provided at the lower end of stiffener. A crack developed in the plate from the web-side toe of the fillet weld deposited between the stiffener and the web around the scallop at the lower end, as shown in Fig. 6 in Poster. After it grew in the web along the toe of corner fillet weld to some extent, it turned to the horizontal direction, extending as far as 10 cm at most, penetrating the web plate. The observation of actual bridges revealed a relative transverse displacement between the web and the lower flange due to various causes. The web plate may be forcibly subjected to repetition of out-of-plane bending of less than 10 Hz. in frequency due to the train axle loading on the girder, and also the web plate vibrates in its natural frequency of 20 to 50 Hz. as seen in Fig.V.

Based on an analysis it was found that the latter relatively more contributed to the fatigue effect on the critical part than the former. Because this kind of crack grows very slowly, not exceeding 10 cm or so in length, and the direction of the crack is parallel to the primary stress of the girder, it seems practically harmless.

For the repair work, usually, a holes were drilled at the tips of cracks and plates or angle steels were attached to that part by high-strength bolts, as shown in Fig. 7 in Poster. It will be effective that the lower end of the vertical stiffener is fixed by some means such as high-strength bolts, which will not so much reduce the fatigue strength of the tension flange.

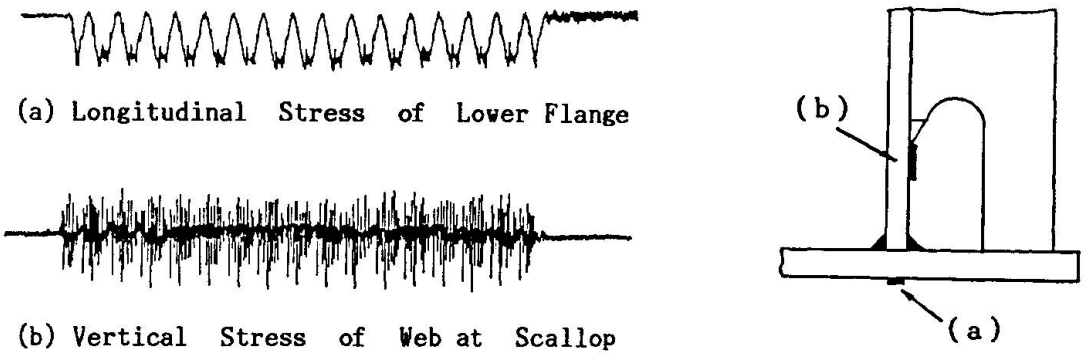

Fig. V Stress Variations of Lower Flange and Web at Scallop

5. Conclusions

The number of occurrence of actual fatigue cracks is rather small and no fatal accident has yet taken place, because important parts of primary members of railway bridges have been designed and manufactured according to specifications where fatigue is taken into account, and fatigue cracks have been discovered before it grew to a serious extent by a well-organized inspection system and proper measures have been taken. However, careful inspection should be continued because new kinds of fatigue cracks may appear in the future.

By Hidehiko Abe, Professor, University of Utsunomiya, JAPAN
Kenji Sakamoto, Senior Engineer, Structure Design Office,
Japanese National Railways
Makoto Abe, Design Engineer, Ditto.

VIBRATION TEST OF OHNARUTO BRIDGE TO CONFIRM WINDPROOFNESS

Honshu-Shikoku Bridge Authority

OUTLINE OF OHNARUTO BRIDGE

Ohnaruto Br.(Fig.-1) is a suspension bridge with the main span and total length of 876m and 1629m. The bridge is a highway-railway combined bridge with double-deck structure (Fig.-2), but it has been temporarily put into service for only highway since June, 1985.

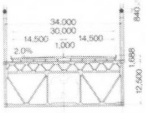

Fig.-2 Stiffening Truss Cross-section

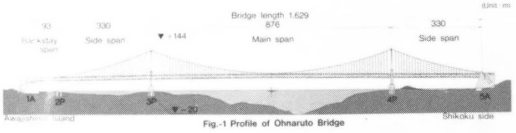

Fig.-1 Profile of Ohnaruto Bridge

WIND-PROOF DESIGN OF OHNARUTO BRIDGE

In the Honshu-Shikoku Bridge Standard for Wind-proof Design, a bridge is to be designed against the design wind speed (V_D), which is derived from the basic wind speed V_{10} (10 minutes average speed at 10m above the sea level) and the height and scale of the structure. V_{10} is expected to have the return period of 150years. Since Ohnaruto Br. is constructed in one of the most windy spots in Japan, V_{10} is determined 50m/s. So, V_D for the suspended structure, for example, is set as 73.0m/s. In addition, the design standard requires wind tunnel test to confirm whether the scheme which is statically designed against V_D have sufficient aerodynamic stability. The logarithmic structural damping for this wind tunnel test was determined by reference to a few previous measurements of long span suspension bridges under small amplitude oscillation or of small or medium span suspension bridges ; namely the decrement for an entire suspension bridge with stiffening truss has been set as 0.03.

VIBRATION TEST OF OHNARUTO BRIDGE

Vibration test was planned mainly to assure the aerodynamic stability of Ohnaruto Br. by observing the oscillatory characteristics such as decrement, mode etc. at large amplitude similar to the reference amplitude (at which the decrement for wind tunnel test shall be fixed, namely 0.5 deg. for the torsional mode). To vibrate the actual bridge to such large amplitude, vibrators (Fig.-3) capable of producing large oscillatory force even at low frequency were developed and assembled. The oscillation of the suspended structure was observed mainly by accelerometers.

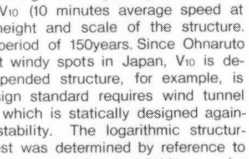

Fig.-3 Vibrator

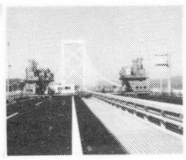

Vibrators at middle span

As the results, the followings were concluded. (1) The observed damping at large amplitude of the first symmetrical torsional mode during the free oscillation was 0.033, slightly higher than 0.03 which was specified in the design standard. The observed damping of the other modes was also higher, thus the damping used in wind tunnel test was concluded to be appropriate (Fig.-4,5 & 6). (2) The observed natural frequency for all test modes was also slightly higher than the calculated value, thus the frequency used in wind tunnel test was concluded to be appropriate, too (Fig.-7 and Tab.-1). From the above mentioned results, the quality of the wind-proofness of Ohnaruto Br. was assured.

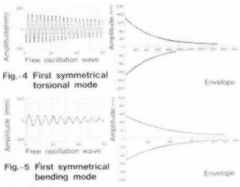

Fig.-4 First symmetrical torsional mode

Fig.-5 First symmetrical bending mode

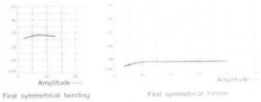

Fig.-6 Logarithmic decrement

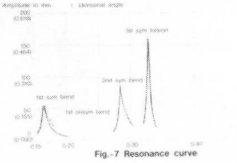

Fig.-7 Resonance curve

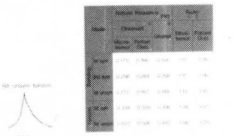

Tab.-1 Comparison of natural frequency

Vibration Test of Ohnaruto Bridge to Confirm Wind-Proofness

I. OKAUCHI
Professor, Chuo University
Japan

A. TANAKA
Honshu-Shikoku Bridge Authority
Japan

K. IWAYA
Honshu-Shikoku Bridge Authority
Japan

N. FURUYA
Honshu-Shikoku Bridge Authority
Japan

1. Introduction

These experiments were significant such that two essential parameters for the windproof design by wind tunnels of large suspension bridges (decrement, natural frequency), were verified by applying large amplitude vibrations to an actual long span bridge (Ohnaruto Bridge). A summary of this report has already been described in the photo to be shown in the latter part. However, we feel that there may be places where the contents are indecipherable, so we decided to present the results again with some supplemental explanation.

Also, a flowchart of the windproof design of the Honshu-Shikoku Bridges, intensity of wind, magnitude of amplitude, and comparison table of decrement by mode of vibration, are newly added.

2. Windproof design of the Honshu-Shikoku Bridges

In the windproof design of the Honshu-Shikoku Bridges, the cross section obtained by the static design through the process shown in Fig.-2 must be verified dynamically using a wind tunnel test. The structural decrement to be used in this dynamic verification was determined with reference to actually measured examples of existing suspension bridges by means of small amplitudes. For the dynamic verification of a suspension bridge having a stiffening truss, the logarithmic decrement was assumed to be $\delta = 0.03$, and the cross-section was selected so as not to cause a flutter of larger than 1^{o} of single amplitude up to the wind velocity of 1.2 V_D (1.2 x design velocity) in a uniform wind flow.

3. Vibration experiments an Ohnaruto Bridge.

The experiments were performed for the purpose of verifying the total design rigidity of the suspension bridge by measuring the structural decrement provided for in the "windproof design standards" of the Honshu-Shikoku Bridges as mentioned earlier using a large amplitude near the standard amplitude (torsional angle of 0.5^{o}, single amplitude of about 15 cm) and by verifying the adequacy of the decrement and the frequency of vibration.

To achieve the purpose of these experiments, it was necessary to develop large scale vibrators for low frequency use. The mechanism and various data of the vibrators are shown in Fig-3.

To obtain vibrations of symmetrical and asymmetrical modes, the experiments were performed by placing the vibrator at the 1/2 point and 1/4 points of the center span, and the vibration behaviors of the girder were mainly measured by an accelerograph.

The vibration experiments were performed on the constant micromotion due to wind and on the forced oscillation and free vibration by means of the vibrator. Figs.-4 ~ 7 and Tables-1 ~ 2 show the results thereof.

From the results of the vibration experiments the following were verified:

(1) By comparing the results of the decrement obtained using three different methods, the value obtained during a large amplitude free vibration was largest. It can be seen that the decrement during the free vibration of the amplitude of about 2.0 cm or less tended to decrease but seemed to be constant above this amplitude.

The decrement of the first symmetrical torsional large amplitude free vibration was found to be 0.033, slightly exceeding the decrement of 0.03 for the wind tunnel test as provided for in the "windproof design standards". It was also found to exceed it in the other modes. Therefore, it is judged that the assumption made in the wind tunnel test was adequate for the decrement.

(2) As for the natural frequency, the comparison of the actually measured values and the calculated values is approximately the same, the actually measured values exceeding the calculated values in all vibration modes. Therefore, it is also judged that the assumption made in the case of the wind tunnel test was adequate for the natural frequency.

From the above it can be judged that the reliability of the results of the wind tunnel test performed on the Ohnaruto Bridge has been increased.

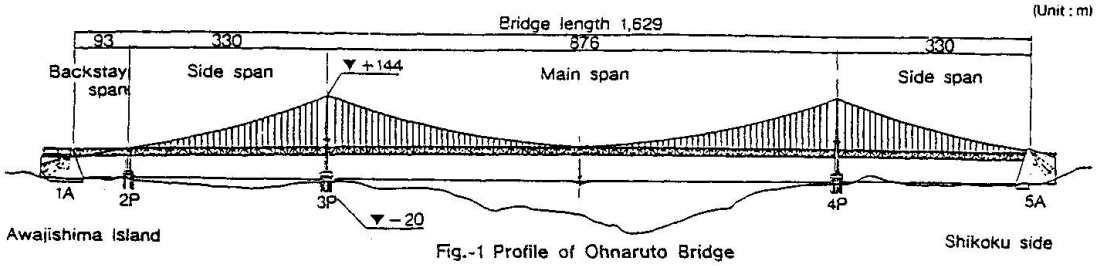

Fig.-1 Profile of Ohnaruto Bridge

Mode		Natural frequency (Hz) Observed ① Micro-tremor	Observed ① Forced Osci.	Calculated ②	Ratio ①/② Micro-tremor	Ratio ①/② Forced Osci.
Bending	1st sym	0.173	0.166	0.154	1.12	1.08
	2nd sym	0.298	0.284	0.268	1.11	1.06
	1st unsym	0.172	0.167	0.149	1.15	1.10
Torsion	1st sym	0.334	0.328	0.306	1.09	1.07
	1st unsym	0.527	0.506	0.497	1.06	1.03

Tab-1 Comparison of natural frequency

Method of experiment / Vibration mode	Constant micromotion: Weak wind (V = 7 m/s, SW)	Constant micromotion: Strong wind (V = 16 m/s, S)	Forced oscillation	Free Vibration: small amplitude smaller than 0.3 - 0.5 cm	Free Vibration: large amplitude larger than 2 cm
First symmetrical bending mode	0.075	0.078	0.097	0.086	0.112
Second symmetrical bending mode	-	-	0.064	0.063	0.080
First anti-symmetrical bending mode	-	-	-	0.082	0.109
First symmetrical torsinal mode	0.025	0.023	0.031	0.018	0.033
First anti-symmetrical torsional mode	0.027	0.025	0.040	0.045	0.057

Table-2 Comparison of Decrement

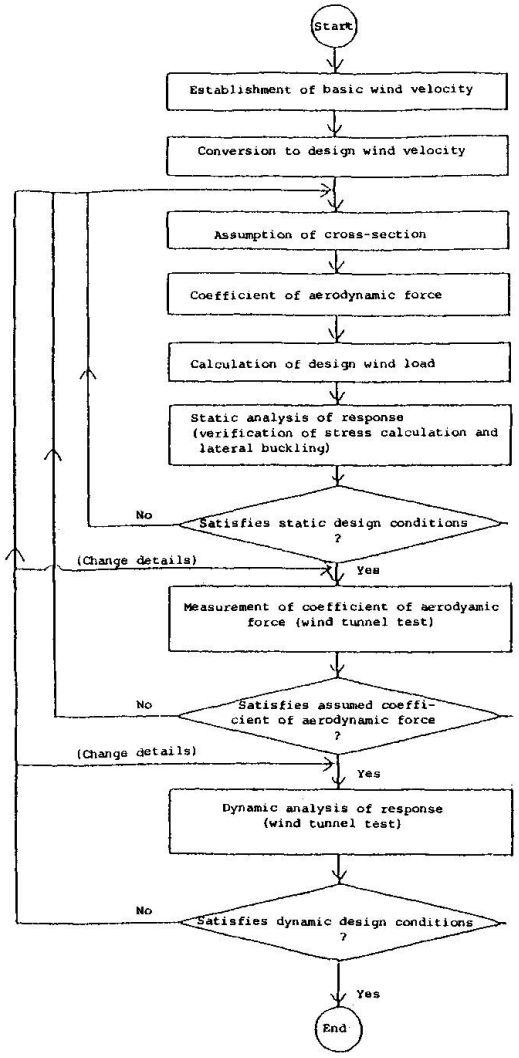

Fig-2 Flowchart of Windproof Design of Ohnaruto Bridge

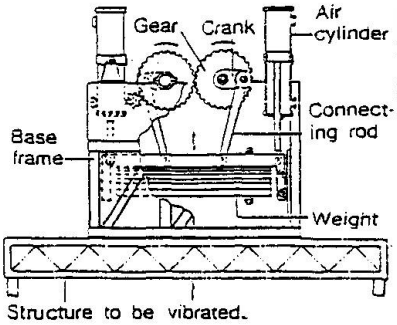

Total weight	Approx. 90 tonvset
Dimension	H=6.30m W=6.10m L=7.10m
Weight of weight	33 ton
Weight stroke	±0.50 m
Vibrating frequency	0.1 Hz–0.6 Hz
Vibrating wave shape	Approx. sine curve
Vibrating force	Max. 196 N (0.5 Hz)
Power	Commercial electricity 440 V, 60 Hz

Fig. 3 Vibrator

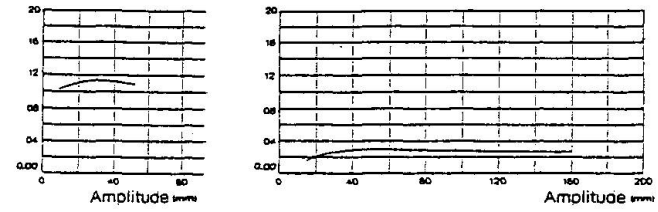

First symmetrical bending First symmetrical torsion

Fig.-4 Logarithmic decrement

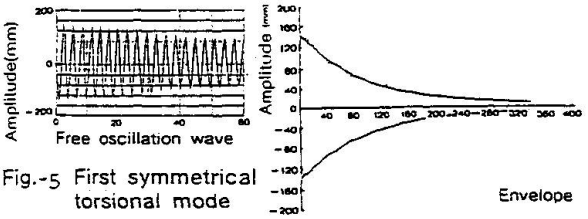

Fig.-5 First symmetrical torsional mode

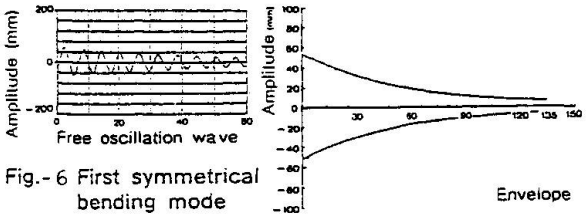

Fig.-6 First symmetrical bending mode

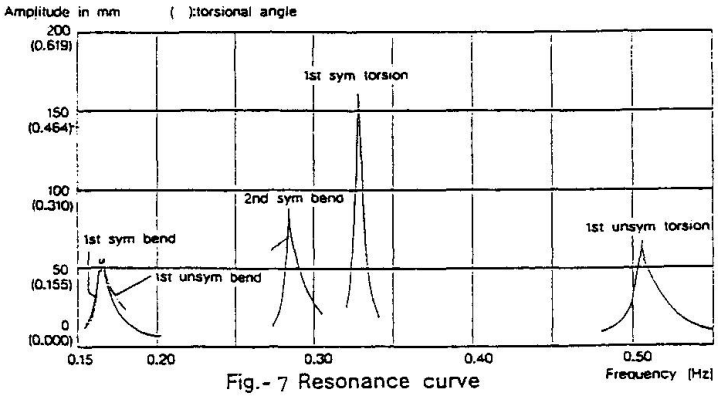

Fig.-7 Resonance curve

NIPPON STEEL

Construction Technology of Cables for Suspension Bridges

Nippon Steel Corporation

Cable Construction of Ohnaruto Bridge

Quality-Oriented Results

(1) Sag and Tower Displacement Survey Deviation

Laser measurement equipment was used to survey sag and tower displacement on Ohnaruto Bridge. Compared to tansits and other conventional optical measuring equipment, this approach provided longer sightline distance when surveying at night, thereby ensuring sufficient precision.

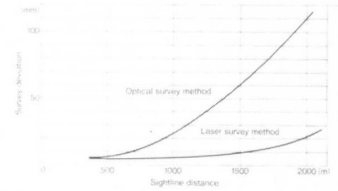

(2) Cable Sag Measurement Results

Entries without unit markings are mm

Timing	1A–2P (Backstay Span)		2P–3P (Side Span)		3P–4P (Center Span)		4P–5A (Side Span)	
	N	S	N	S	N	S	N	S
Targeted Sag Value	0.842(m)		10.820(m)		14.732(m)		10.820(m)	
At Erection of Guide Strand (Sag Allowance)	5mm ± 60	4mm ± 60	6mm ± 80	26mm ± 80	18mm ± 60	14mm ± 60	20mm ± 80	10mm ± 80
When Squeezing is Complete (at Cable Center)	96	128	107	86	39	81	57	75
Innoshima Bridge Results (When Presqueezing is Complete)			59	27	53	90	116	75

Impact of Relative Sag Deviation on Cable Stress

		Relative Sag Deviation among Strands δf	Δf/Δ1	Cable Stress Deviation δσ	Average of δσ (kg/mm²) Ohnaruto Bridge	Kanmon Bridge
Side Span	2P S	7.6mm	5.765	0.06kg/mm	0.10	0.13
	3P N	9.9		0.10		
	3P S	12.6		0.13		
	4A N	7.8		0.08		
Center Span	S	8.2	2.232	0.08	0.08	0.12
	N	8.3		0.08		

(3) Cable Percentage of Void After Cable Band Bolt Tightening

Bridge	Cable Diameter (mm)	Erection Method	Void Ratio of Cable	
			Plan(%)	Result(%)
George Washington	911	AS	20.9	21.2
Golden Gate	919	〃	19.0	17.4
Tacoma Narrows	514	〃		17.2
Forth Road	603	〃	20.8	18.9
Salazar	586	〃	16.8	20.8
New Port	387	PS	18.5	16.7
Kanmon Bridge	664	〃	19.0	16.8
Hirado Bridge	368	AS	20.0	21.2
Innoshima Bridge	610	PS	17.0	17.2
Ohnaruto Bridge	**829**	**PS**	**18.0**	**17.6**

Specification of the Ohnaruto Bridge Cable

Galvanized Wire	Diameter	5.37mm
	Tensile Strength	160~180kg/mm²
Strand	Amount of Wires Consisting Strand	PWS 127
	Unit Weight	22.525kg/m
	Length	1722m
	Weight of Strand	39.0t
Cable	Amount of Strands Consisting Cable	154
	Diameter	840mm
	Amount of Wires Consisting Cable	19,558
	Total weight	11,962t

Arrangement of Cable Strand

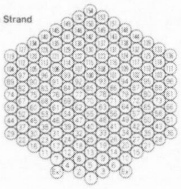

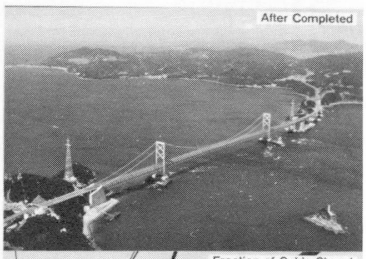

Leere Seite
Blank page
Page vide

Outline of Minami-Bisan-Seto Bridge
Weight (Truss) 39,260ton
(Cable) 23,840
(Tower) 18,990
Total 82,090

CONSTRUCTION OF SUSPENSION BRIDGE

Honshu-Shikoku Bridge Authority

Erection of tower
Compressive force of tower shaft is designed to be transmitted by friction bolt and direct metal contacts by 50% each.
To assure this designe policy, end surface of three blocks of tower shaft was finished by facing machine. At the erection site the ratio of metal contacts was inspected using gap gauge, and the ratio was confirmed at inspected points.

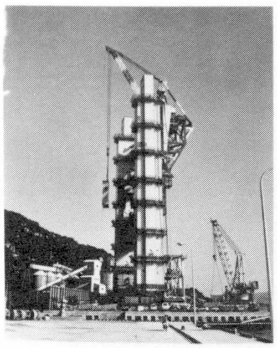

Erection of tower

Erection of cable
To control the accuracy of main cable of suspension bridge, it is important to adjust the length of each strand.
In fabrication, the length of each strand is determined by the gauge wire which was measured correctly. At the site, the hight of 1st strand was measured careflly and adjusted to the right position.
The hight of other strands were adjusted to this standard strand. These adjustment should be done at around midnight when the temperature of each strand were uniform. The void ratio of main cables, which indicates how the wires were compacted, are within 20% as specified.

Erection of cable

Erection of suspended structure
To erect the stiffening truss, the panel members which is assembled at the shop are connected tightly each other so as to keep stiffness of erected truss. When the stiffening truss is connected to the suspended ropes, oil jacks are set at three panel points for each side of truss in order to distribute the tensile force of suspended ropes. At several steps during erection, the hight, torsional deflection, and others will be measured to confirm the accuracy comparing measurement and calculation.

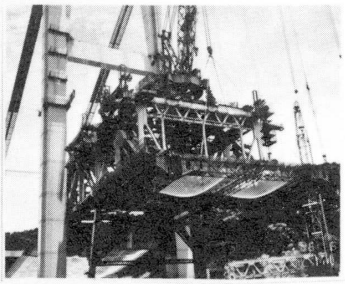

Erection of stiffening truss

Construction of Suspension Bridge in Honshu-Shikoku Bridges Project

I. YOSHIDA
Honshu-Shikoku Bridge Authority
Japan

K. TADA
Honshu-Shikoku Bridge Authority
Japan

M. NARUI
Honshu-Shikoku Bridge Authority
Japan

Y. KISHIMOTO
Honshu-Shikoku Bridge Authority
Japan

1. Introduction

There are eleven suspension bridges to be constructed in the three routes of the Honshu-Shikoku Bridges project. Of these, the Akashi-Kaikyo Bridge of the Kobe-Naruto route and the six suspension bridges of the Imabari-Onomichi route are for highway use only, while the other suspension bridges are for combined highway and railway use. The Ohnaruto Bridge is designed to allow the passage of Shinkansen trains in the future. The three suspension bridges of the Kojima-Sakaide route are also designed to allow the passage of Shinkansen and ordinary type trains. However, only ordinary type trains are scheduled to be constructed at the present stage.

2. Construction of Superstructures of Suspension Bridges

(1) Tower Construction

1) Tower fabrication

All towers for the suspension bridges of the Honshu-Shikoku Bridges Project are made of steel. The towers are divided into blocks of about 10m length, each block being constructed of three cells. At the tower joints friction bolts are used, and the design is such that 50 % of the axial force is transmitted by direct contact with the end faces of the members. To secure this design prerequisite each cell fabricated at the plant was temporarily assembled and finished using an end facing machine.

2) Erection of tower

Prior to the erection of the tower shaft, the surface of the top of the pier was polished using a concrete grinder, to ensure the perpendicularity of the tower when completed.

The erection of each block of the tower and the installation of the various members, such as diagonal members, horizontal members, etc. was performed using a creeper crane which was mounted on a guide rail attached to the tower column already installed. As each block was erected the metal contact ratio was inspected and confirmed for the required quality. Also the perpendicularity was measured and when necessary a correction was made when erecting the next block to offset the previous error.

(2) Construction of cables

1) Wires for cable

For all cables of the suspension bridges parallel wires of about 5 mm in diameter were used. The quality required of this wire is specified in the Honshu-Shikoku Bridge Standards. In strength of wire testing methods for each item and criteria for judgement, etc. are provided. The breaking strength is required to be in the range of 160 kg/mm^2 -180 kg/mm^2. Each wire is galvanized to keep it from corrosion. The diameters of the wires vary depending on the bridge, which is in the range of 5.10 mm to 5.37 mm. In the PWS method, strands consisting of 127 wires are fabricated in the shop. The length of the strand is controlled using a gage wire prefabricated to the required length which is marked and placed at one corner of a regular hexagon. Colored wires are placed on the other corners facilitating inspection of twists in the strand at the site.

2) Installation of cables

There are two methods of constructing cables for a suspension bridge. One is the aerial spinning method (AS method) and the other the prefabricated parallel wire strand method (PWS method). Five of the six suspension bridges constructed to date in the Honshu-Shikoku Bridges Project were constructed using the latter method. The only example of using the AS method was the installation of cables for the Shimotsui-Seto Bridge, in which case the tunnel anchor method was used. If the cable has the same number of wires the area for connection can be made more compact, which was the reson that the AS method was used.

It is important that the cables for suspension bridges be installed at the required height, as this governs the configuration of the bridge when it is completed. However, the height of the cables cannot be adjusted after all the strands are installed, therefore surveys and adjustments were made during the installation of the strands to insure the accuracy of the bridge height when completed. To make sure the first strand was installed at the required height a survey was conducted and necessary adjustment was made, which was performed by sliding the strand at the saddle of the tower or the anchorage. Using this first strand as a basis, the height of the second and subsequent strands was adjusted. When about 1/3 and 2/3 of the strands were installed the heights of the cables were surveyed, confirming their accuracy.

The adjustment performed as mentioned above also contributed to the alignment of the strands in the cable, helping to meet the required void ratio for the cable after clamping.

The maximum void ratio of the cable is specified at about 20%. The larger the ratio, the more wires are crossed, suggesting that there may be a possibility that the strength at the crossing will become lower.

(3) Construction of girder

1) Structure of stiffening girder

The stiffening girders of the suspension bridges of the Honshu-Shikoku Bridges consist of steel trusses, except for one case where a steel box girder is used. This is mainly to increase the

stability against wind. In this regard the sectional configurations of the stiffening girders were determined after wind tunnel tests had been performed.

2) Erection of stiffening girder

There are two methods of installing stiffening girders for suspension bridges. One is the method in which the stiffening girder, assembled to a designated length, is directly lifted at the installation location using a lifting device attached to the cables, i.e. the block erection method. The other is the method in which individual members are installed in sequence by overhanging from the towers to the right and left. In general, the former is considered advantageous, however, in the light of the situation that the straits across which the Honshu-Shikoku Bridges are to be constructed are congested navigation routes and the use of sea surface below the girder is limited, most of the bridges of the Honshu-Shikoku Bridges Project use the latter method.

The controlling of the configuration of the stiffening girder is accomplished by test assembling it in the shop and confirming the accuracy of the dimensions of each members. At the site various surveys (displacement, torsion, stress conditions, etc.) are performed at several steps during erection and confirmation of the installation accuracy is made. Under normal conditions, however, no adjustment would be required at the site as no significant errors can occur during the erection.

(4) Conclusion

The quality control in the construction of suspension bridges can be classified roughly into three items, as follows:

- o Quality control of materials used---strengths of steel materials, thickness and flatness of steel plates, quality of point, etc.
- o Quality control in shop fabrication ---accuracy of dimensions of members, inspection of welding, working conditions and thickness control of painting, etc.
- o Quality control at the construction site--- measurement of configuration when installed, etc.

To ensure the quality of an overall bridge it is important to confirm that at all these stages the required standards as provided for in the HBS are met. This importance must be emphasized in the light of the fact that once the work proceeds to the next stage there are many items that can no longer be corrected.

Outline of Iwakurojima
Cable-stayed Bridge
Weight (Tower) 8,340ton
(Cable) 2,230
(Girder) 24,530
Total 35,100

CONSTRUCTION OF CABLE-STAYED BRIDGE

Honshu-Shikoku Bridge Authority

Erection work and Quality control

Field quality control for erection of girder and stay cable is roughly classified into followings

(1) Quality control of welded joints

Field welding quality control is classified as follows

-Welding procedure test under similar conditions to actual erection site.

-Control of welding conditions and groove geometry

-Inspections by N.D.T (X-ray and P.T.)

(2) Erection accuracy control

Regarding bolted joints, the pilot holes into which drift pins are driven during shop assembly are used in erection of main truss at the site to reproduce the figures in shop.

(3) Configurations and stress measurement

To confirm accuracy during erection and after completion, configuration and stress are measured on following items, girder figure, cable tension, tower tilt, girder stress, and support reaction.

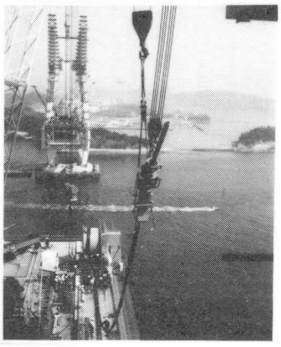

Erection of cable

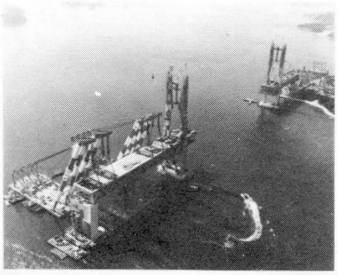

Erection of large block

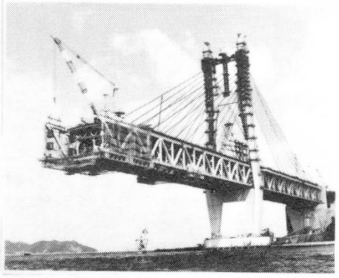

Erection of main truss

Construction of Cable Stayed Bridges in Honshu-Shikoku Bridges Project

M. MATSUZAKI
Honshu-Shikoku Bridge Authority
Japan

T. OHMACHI
Honshu-Shikoku Bridge Authority
Japan

M. YASUDA
Honshu-Shikoku Bridge Authority
Japan

T. OHTA
Honshu-Shikoku Bridge Authority
Japan

1. Control of erection accuracy

The control method for erection accuracy is described in another paper of this final report. (c.f. Quality Control at Erection Site of Iwakurojima Bridge.)

2. Field welding of steel deck

As this bridge employs the composite steel deck, and joining of the steel deck was performed by field welding, it was considered possible that contraction due to welding could affect the erection accuracy of the main girder. The erection of the main girder was performed by use of the "bolt hole control method to secure sufficient accuracy. Therefore, when examining the root opening measured for the purpose of quality control of welding, the difference in values between the site and the shop could be considered to be due to the contraction as a result of welding, and of root detection errors. Therefore, the verification of the effect on the main girder camber due to the contraction of field welding based on the value of the root opening is performed, as follows:

(1) Comparison of root opening difference between shop assmbly and construction site.

Fig-1 shows the root opening in the shop and on site.

Apparently the transverse root opening in the site bridge axis is larger than that in the shop. This is a result of the welding contruction, because the drift pins and the temporary bolts at the bolt joints between the main girder and the steel deckplate were removed, releasing the residual stress caused by welding. Therefore the main girder camber was not greatly affected by the contraction due to the welding.

The longitudinal root opening tends to be smaller at site than in the shop, although the difference is small.

Also the longitudinal root opening did not appear to have any effect on the width of the main girder because stress releasing was performed as in the case of the transverse opening, with the floor truss keeping the width of the main truss.

(2) Quality of welds (Fig-1)

33 - 46 show larger root openings than 19 - 32. This is due to the fact that the standard values of the root opening differ depending on the method of welding (Submerged arc welding-CO_2 gas automatic arc welding).

The transverse root openings in the direction at right angles to the bridge axis were larger at the site, but the results of X-ray tests show that the quality of welding was satisfactory, presenting no problems.

3. Girder configuration and cable tension at the time of closure

Fig-2 shows errors between the planned values and the measured values at the time of closure of the girder. In the figure, the planned values were calculated according to the loading at the time. The error at the center of the central span is + 34 mm and that on the side spans is - 34 mm, and the tolerance on the central span being 118 mm and 59 mm on the side spans, respectively. These prove that the accuracy is satisfactory.

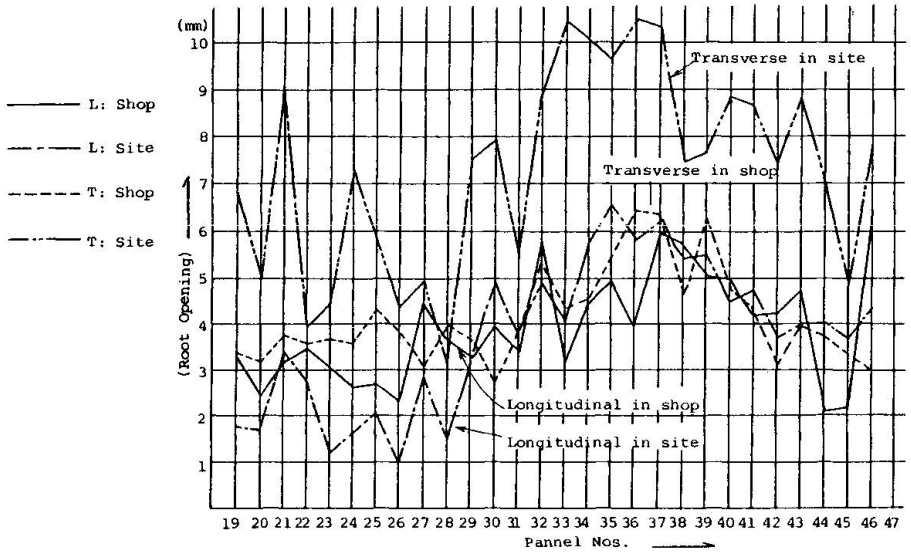

Fig. 1 Root Opening Difference between Shop Assembly and Construction Site

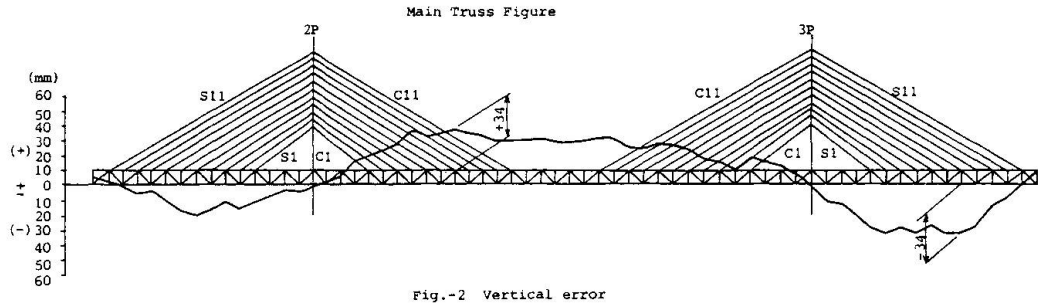

Fig.-2 Vertical error

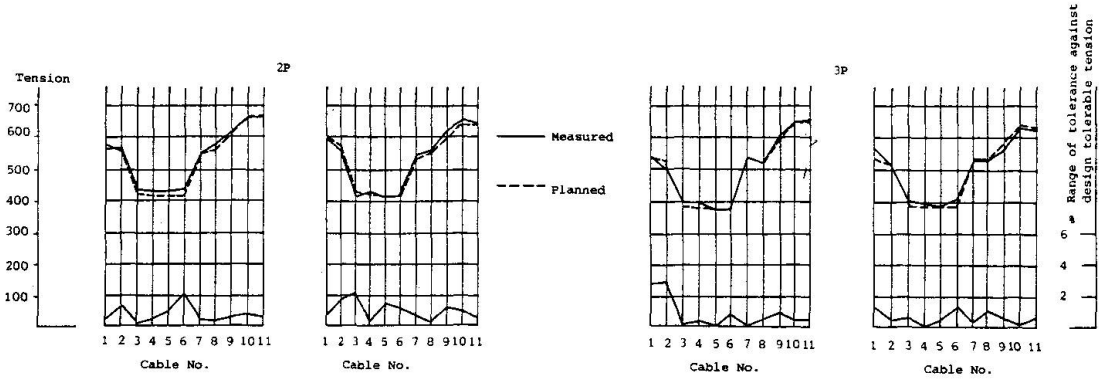

Fig. -3 Cable Tensions

Fig-3 shows cable tensions at each tier at the time of closure. The difference between the planned value and measured value according to the loading condition at the time was smaller than 5%, showing that the erection was performed with an extremely high accuracy.

However, as the allowed designed erection error was ±5% of the allowable design tension at the time of completion, it is judged that the range of errors at this stage was to be made ±2,8% of the allowable tension, taking into account the errors in the measurement. Therefore, shim plate adjustment was performed only on the cables at the 6th tier of the left side span, and at the 2nd tier and 1st tier on the right side of the center span.

4. Measurement of stress

At each point of measurement a strain gauge was attached and the stresses at each erection stage were measured. The axial forces were calculated from these values and the planned values were compared. Fig-4 shows the condition of the axial force acting near the tower columm on the 2P side. The axial force of the upper chord member of the composite steel deck plate is the resultant force of the axial force of the chord member alone and the axial force of the steel deck, but the difference in calculation between the planned value and the measured value is deemed to have resulted from the fact that the stress in the steel deck-plate includes the bending stress of the direct loading of erection machines, etc. However, since the values for the lower chord member match with the planned values, the erection can be judged to have been completed with a satisfactory accuracy.

5. Conclusion

It is judged that the contraction caused by field welding was thoroughly released by arranging the welding sequence and by releasing the stress by removing the drift pins and temporary bolts etc. In addition, thanks to the bolt hole control method, which aims at the reproduction of the shop assembling accuracy at the site, a high erection accuracy was obtained without having to adjust the cable shim and the camber during erection.

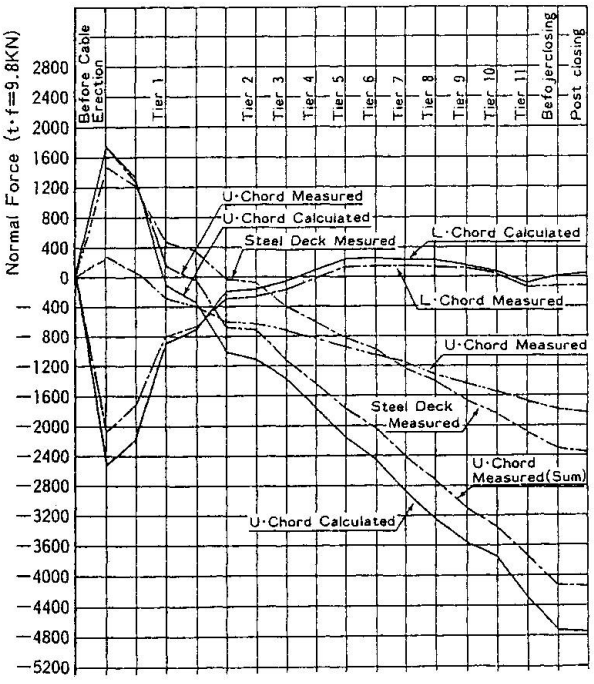

Fig-4 Trasition of Main Truss Stress

Outline of Yoshima Bridge
Weight(Truss) 15,540 ton
(Floor system) 5,510
(Others) 4,050
Total 25,100

CONSTRUCTION OF YOSHIMA BRIDGE

Honshu-Shikoku Bridge Authority

The main truss of Yoshima bridge was erected by two methods. For the 1st step, large block was erected using floating crane on the intermediate support.
Other members were erected by balanced cantilever method. These methods were adopted considering topographic condition and limitation of carrying capacity of floating crane.
As a result of this method, the fabrication error and erection error will be accumulated to the closing panel at the center of span. Therefore,

(1) The relative location of both end of erected truss will be adjusted by compulsive force.
And this force was taken into consideration in designed stress of the members.

(2) High accuracy of members was required in fabrication.
Especially the gap of splicing in lower chord members is specified to be within 1mm, and metal contacts for the members at the intermediate support.

(3) The bridge configuration and the axial force of temporary diaganal support were measured to confirm that erection work was carried out as planned.

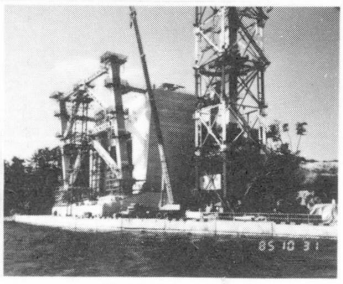

Temporary support

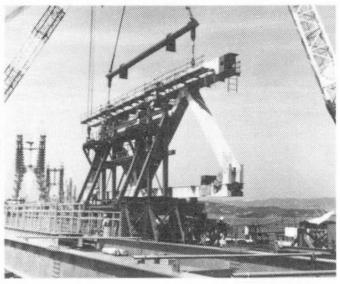
Carrying of members

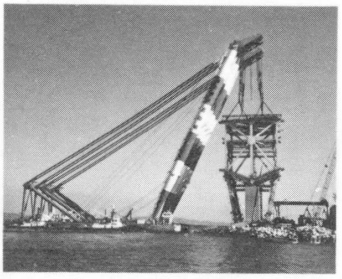
Erection of Large Block

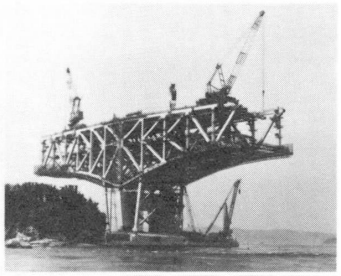
Cantilever method

Construction of Truss Bridges in Honshu-Shikoku Bridge Project (The Yoshima Bridge)

K. SAEKI
Honshu-Shikoku Bridge Authority
Japan

J. HIRAYAMA
Honshu-Shikoku Bridge Authority
Japan

K. IIJIMA
Honshu-Shikoku Bridge Authority
Japan

H. OHASHI
Honshu-Shikoku Bridge Authority
Japan

1. Bridge Description

The Yoshima Bridge (cf. Fig.1) is a continuous 3-span truss bridge with a total length of 585 m (175 m + 245 m + 165 m) for combined highway and railroad use, forming part of the Honshu-Shikoku Bridge Project. Due to the route alignment, an S-shaped transition curve is included in the bridge, which connects with suspension and cable-stayed bridges at both ends. This makes the design, fabrication and erection of this bridge particularly complicated because the main trusses should be knuckled at the intermediate piers and the main trusses of the side spans are not arranged parallel to the central span.

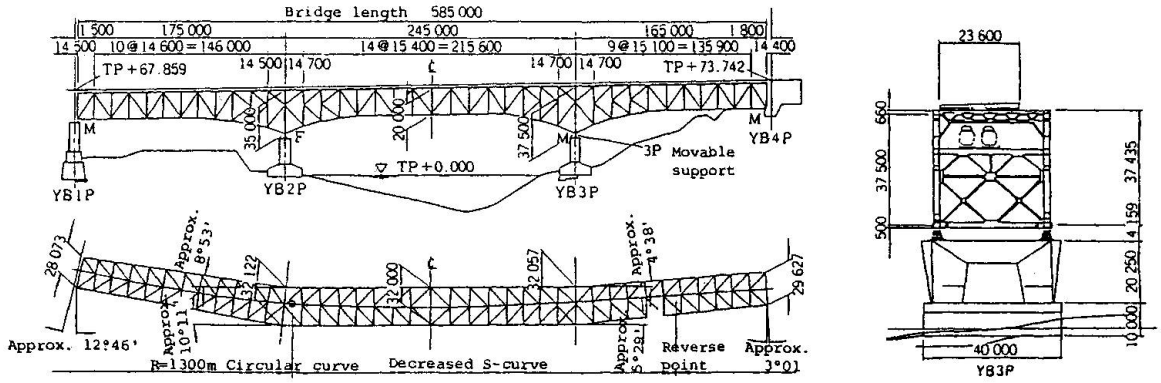

Fig. 1

Various loading combinations were considered in the design, and the safety of running trains was checked by simulation.

The live loads are vehicular loads (4-lane) and train loads (4-track) both of which are the dominant loads in the design. Also wind loads for a wind velocity of 68 m/sec and inertia forces due to earthquakes (magnitude of 8 in Richter scale) computed by dynamic analysis were applied.

High-tensile strength steels up to HT80 (breaking strength of 80 kg/mm^{2}f) are extensively used for the main structure. The standard chord section is 1.48 m x 1.4 m.

The bearings of this bridge are the largest in the project, to support the reaction of 11,000 tonf.

2. Accuracy control and measures against possible erection errors

The erection of the bridge was carried out by the procedure shown in Fig. 2.

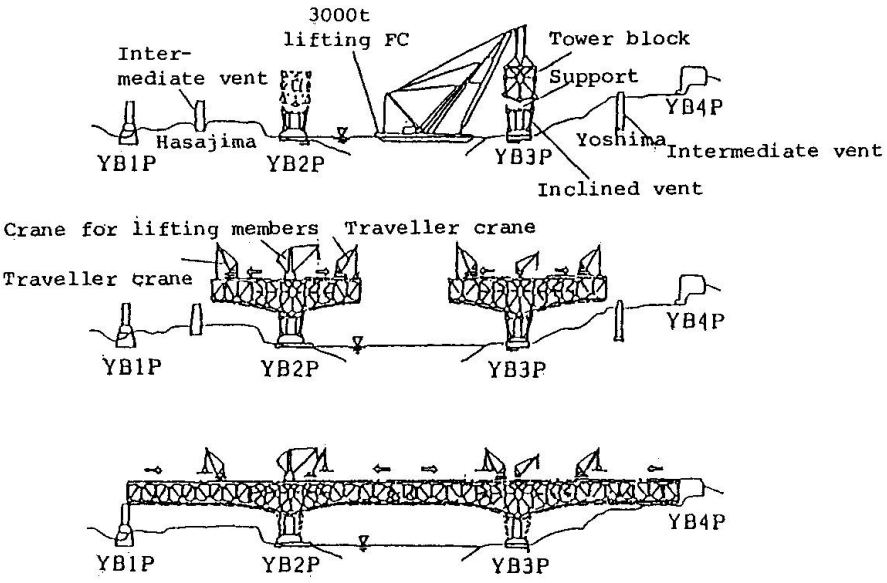

Fig. 2

Firstly, large two-panel, prefabricated blocks were installed on the middle piers by use of a 3,500 tonf lifting capacity floating crane, then each individual member was erected by the cantilever method, maintaining the balance on both sides.

Because of the complexity of the structure of the bridge, a higher precision was required for the fabrication, and measures against possible closure errors were considered in the design, some of which are described as follows.

1 The accuracy of the camber computation was greatly increased by an analysis using a 3-dimensional model which represented all members of the main trusses and laterals.

2 The fabrication precision for the two-panel blocks which govern the initial orientation of the successive single member erection was extremely accurately set, as the distance between the trusses was to be less than 5 mm.

3 The fabrication precision of chord members was accurately specified as each gap at the joint between lower chords had to be less than 1 mm.

4 Most members were fully assembled in the shop and base holes were used during the erection to ensure the accuracy.

5 Compulsory forces would be applied at the closure of the main truss.

In the design, the forced displacements in the horizontal, vertical and rotational directions were 50 mm.

The bridge was closed very successfully on the 13th September, 10 months after the first block was installed.

Total Weight of Quenched and Tempered High-Strength Steel: 21,000 ton

Total Length of Exermined Corner Weld of Main Truss Chord Members : 58,000m (3 Suspension Bridges and 2 Cable Stayed Bridges in Kojima-Sakaide Route of Honshu-Shikoku Bridges)

Quality Requirement of Corner Weld of Truss Chord Members

Honshu-Shikoku Bridge Authority

The Honshu-Shikoku Bridges include many long, large bridges for combination road/railway use that use a great deal of quenched and tempered high-strength steel which was previously not often used in railway bridges. Also, in the particular case of stiffening girders of suspension bridges, since the ratio of the live load stress was greater, close examinations were carefully conducted as to the fatigue due to repeated loading of trains. As one of such examinations, a large-scale fatigue test was carried out on approximately one-third models of the truss panel (Photo 1). As a result, it was found that the fatigue strength would be reduced by reason of the micro welding defects, such as blowholes in the corner joints of box-section members.

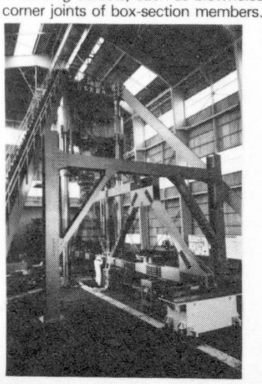

Photo 1 Large Scale Fatigue TEST

Following the aforementioned a relationship between the blowhole dimensions and the fatigue life was found, based on the test results and calculation by fracture mechanics (see Fig. 1). By comparing the results with the design fatigue-life curves allowable dimensions for blowholes has now been determined, considering the working stress (Table 1).

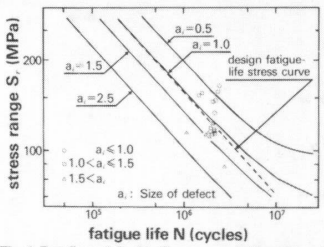

Fig. 1. Predicted S_r–N_f Curves and Test Results

Table–1 Quality Requirements

Classification / Size of defect	Special A Member	A Member	B Member	Remarks
Minor axis (mm) (W size)	1.5	3.0	6.0	H, W
Major axis (mm) (H size)	1.0	6.0	6.0	
σ_r / σ_a	0.7≤	0.5~0.7	0.5>	

σ_r: Working stress range
σ_a: Allowable stress range

During fabrication, all possible occurrence of welding defects has been avoided, by carrying out severe control in welding condition, root gap, cleanliness of the groove face, and so on. Moreover, the suitability of fabricating conditions has been efficiently confirmed, by making actual-sized pilot members prior to the fabrication of the members. At the same time, a nondestructive examination was performed by means of automatic ultrasonic equipment (Photo 2), and when any defects of greater dimensions than the allowable ones were detected, they were soon repaired.

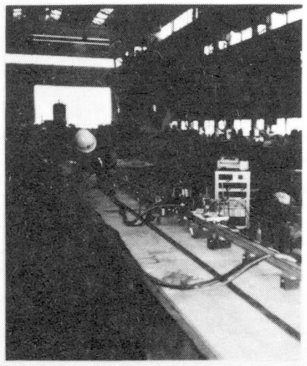

Photo 2 Nondestructive Examination

Quality Requirement of Corner Welds of Truss Chord Members

J. TAJIMA
Professor, Saitama University
Japan

K. YAMAGUCHI
Honshu-Shikoku Bridge Authority
Japan

M. NARUI
Honshu-Shikoku Bridge Authority
Japan

R. TORIUMI
Honshu-Shikoku Bridge Authority
Japan

1. Introduction

As the Honshu-Shikoku Bridges consist of many large bridges for combined highway and railway use and which use an enormous quantity of quenched and tempered high strength steels that have not often before been used for railway bridges, it was important to examine the fatigue strength due to the running of trains. As a part of the examination a large scale fatigue test was performed, and as a result, it was found that welding defects in the corner joints of the chord members greatly reduce the fatigue strength. These results were reflected in the design and fabrication of large bridges for combined highway and railway use. This report describes the summary of the process thereof.

2. Examination of fatigue

The Kojima-Sakaide route and the Ohnaruto Bridge of the Honshu-Shikoku Bridges are combined highway and railway use. There are three suspension bridges (span: 230 + 940 + 230, 274 + 990 + 274, 274 + 1,100 + 274 m), two cable stayed bridges (span: 185 + 420 + 185, 185 + 420 + 185 m) and truss bridges in the Kojima-Sakaide route, and the Ohnaruto Bridge also is a suspension bridge (span: 330 + 876 + 330 m). These bridges contain an enormous quantity of quenched and tempered high strength steel (580 - 800 MPa class), reaching as much as 21,000 tons for the suspension and cable stayed bridges of the Kojima-Sakaide route alone. During the planning stage there was insufficient data available on the fatigue tests of quenched and tempered high strength steel, requiring verification of the fatigue strengths of various joints. Taking into account the magnitude of the Honshu-Shikoku Bridges, it was considered necessary to perform the examination considering the size effect, welding conditions, etc. Therefore, a fatigue testing machine, with a maximum dynamic loading of 400 tons, was manufactured and fatigue tests were performed.

This large scale fatigue test was performed using large scale specimens of various joints and partial structural specimens of nearly the same size as the actual members. As a result of the fatigue tests performed on an approximately one-third model of the truss panel (phot 1 in poster), it was verified that the fatigue strength greatly decreases due to welding defects in the corner joints of the chord members, such as root blow-holes, lack of penetration, drooping, etc. Reflecting these results, from the relationship between the fatigue life and defect size calculated based on

the fracture mechanics and from the results of the test, the allowable size of welding defects was determined. (Fig.- 1, Table- 1 in poster).

3. Fabrication

As the allowable welding defect size determined from the test results, etc. was extremely small, the measures to be taken to prevent the welding defects from occurring were examined, the main items of which are as shown below.

1 Thoroughly clean the groove face and adjacent area, and when using a grinder, match the grain of the grinder with the direction of the welding line.

2 When assembling, the root gap must be smaller than 0.5 mm after tack welding.

3 Pay attention to the selection of welding methods and welding conditions such that the tack weld can be completely rewelded and pay attention to the device, etc. used for stable welding condition.

For fabrication, control items and execution procedures were laid down for each fabrication process. Also, prior to the fabrication, a welding test was performed using actual size pilot members and the adequacy of the welding method in meeting the required quality was confirmed.

4. Nondestructive inspection

Nondestructive inspection of the fabricated members was performed and the members were repaired as necessary. An ultra-sonic defect probing device was employed in the nondestructive inspection, as it was difficult to apply the radiograph test because the members have box-shaped sections. However, conventional ultra-sonic defect probing is not aimed at detecting the micro-defects that are subject of this test nor has it the recording capability. Therefore, a new ultra-sonic defect probing system was developed, eight types of which were recognized to have sufficient capability to probe the defects, and these were used for the inspection of members. The required capability was that the system must have an accuracy to detect defects of size W (refer to Table-1 in poster), i.e. = 1.5 mm in diameter with n $\pm$0.8 mm.

An automatic ultra-sonic defect probing system can be operated automatically, and divided into two by the traveling method. One is the type that traces the weld line and the other scans the weld in a zigzag course. Both types use more than one probe, and by adopting the combined use of a vertical probe and an ablique angle probe, in addition to using a focus type probe, an improvement in probing capability was attempted.
Fig-1 shows an example of probe position.

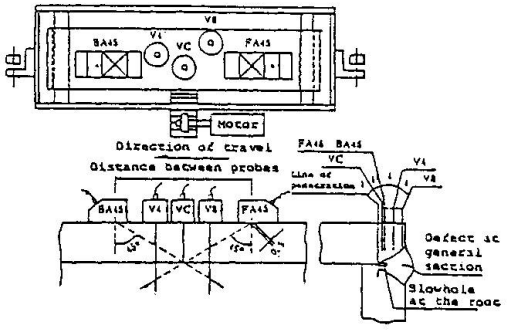

(Example of probe position)

VC	Vertical probe to detect penetration
V4, V8	Vertical probe for general section
FA45	Forward oblique angle probe at the root
BA45	Backward oblique angle probe at the root

Fig-1 Example of probe position

5. Results of fabrication

As an example of the results, Table-1 shows the results of the nondestructive inspection of a cable stayed bridge. The occurrence rate of welding defects was controlled to 0.12 - 0.13/m and they were all micro-defects, allowing us to consider that high quality welding was obtained.

Table-1 Results of Automatic Ultra-sonic Defect Probing

	Stress level	Size of defect							Number of defects per length inspected No./m
		W dimension (mm)			H dimension (mm)				
		0.5 ~ 1.5	1.6 ~ 3.0	3.1 ~	1.0 ~ 2.0	2.1 ~ 4.0	4.1 ~ 6.0	6.1 ~	
Corner weld	Special A	11	2	0	9	1	3	0	$\frac{13}{217} = 0.06$
	A	73	13	1	62	19	6	0	$\frac{87}{610} = 0.14$
	B	19	0	0	7	12	0	0	$\frac{19}{76} = 0.25$
	Total	103	15	1	78	32	9	0	$\frac{119}{903} = 0.13$
Fillet weld	Special A	69	5	0	61	12	1	0	$\frac{74}{217} = 0.34$
	A	26	3	0	26	3	0	0	$\frac{29}{610} = 0.05$
	B	4	3	0	4	1	2	0	$\frac{7}{76} = 0.09$
	Total	99	11	0	91	16	3	0	$\frac{110}{903} = 0.12$

6. Conclusion

As mentioned above the design and fabrication was performed based on the results of the fatigue examination performed in advance. However, the role to be played by the checking and inspection of the bridge after it opens to traffic is considered important. Therfore, while arranging and storing the results of the non-destructive inspection performed at the time of fabrication, so as to create a valuable reference for the maintenance of the bridge, are promoted, the establishment of an inspection system by which a fatigue crack can be detected while it is still small and a method of repairing fatigue cracks are also being promoted.

Outline of Construction,
Total concrete Volume 550000m³
Maximum foundation 230000m³
Number of foundation 11
Maximum depth of sea 50m
Constructed by Honshu-Shikoku Bridge Authority.

QUALITY CONTROL OF PREPACKED CONCRETE FOR LARGE FOUNDATIONS

Honshu-Shikoku Bridge Authority

(1) Prepacked aggregate : The aggregate were washed and classified in the storing base before shipment. Then they were carried to the foundation site and washed and classified again. At filling in, more than one time per day, sieving analysis test and decantation test were taken controlling within 2% pass rate by 80mm sieving analysis test and within 0.03% by decantation test.

Table-1. Quality of poured mortar

Frow value	bleeding rate	Expantion rate	Compresive strength
17.9 SEC	2.0% (3HR)	5.7% (3HR)	319kgf/cm² (28day)

(2) Grouting : In the mortar plant barge, mortar materials were lifted, weighed, mixed and poured into at the rate of 4000l/min under automatic control. Information of grouting was scatterred over the wide range and whose contents is various kinds. During grouting, efforts to collect these data and to operate under the proper judgement should have been made. But as it was imppossible to do all work by hand, the data were displayed on graphic panel, CRT display etc, in the operation room. Grouting mortar was checked per 1000m³ and it resulted favorable value over all items of quality as shown in table 1. Please pay attention to low bleeding rate. Bleeding rate could become so low, because fly ash cement of good quality and sand with controlled particle dia. (FM1.8±0.2) in the storing base were adopted.

(3) Core sampling : After mortar was poured into completely, the cores with 45cm dia. from the base to the top of pier were taken, and these cores (without any material separation phenomeon) could be completely collected at each 5m pre-cut. Moreover, the average compressive strength of age 91 day's was 200kgf/cm².

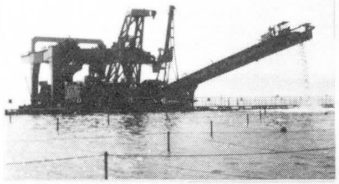

Coarse aggregate

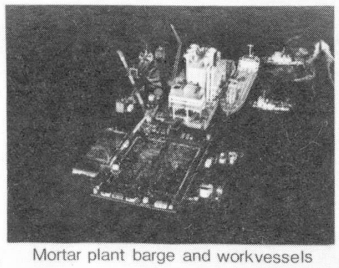

Mortar plant barge and workvessels

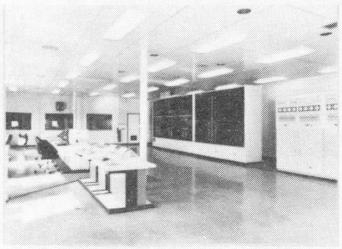

Operation room in the mortar plant barge

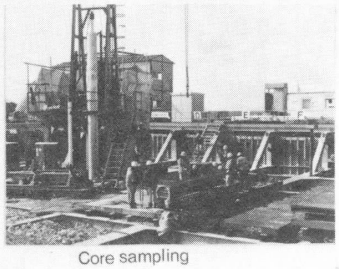

Core sampling

Quality Control of Prepacked Concrete for Large Foundations

A. TAKEYAMA
Honshu-Shikoku Bridge Authority
Japan

N. SAKURAI
Honshu-Shikoku Bridge Authority
Japan

S. KASHIMA
Honshu-Shikoku Bridge Authority
Japan

M. SAKAMOTO
Honshu-Shikoku Bridge Authority
Japan

1. Introduction

Eleven main foundations in the strait for the Kojima-Sakaide route of the Honshu-Shikoku Bridges were constructed using the prepacked concrete method. This report describes the quality control of this prepacked concrete.

2. Summary of Prepacked Concrete

Table-1 shows the foundations which were constructed using the prepacked concrete method. The volume of concrete placed was 540,000 m^3 in total, with the water depth of 10 - 50 m. These foundations were constructed between October 1980 and October 1984. The process of prepacked concrete consists of placing of the coarse aggregates and injection of the mortar. The construction was performed at the high rate of 50,000 m^3/month for aggregate placing and 240 m^3/hr for mortar grouting.

3. Placing of Coarse Aggregate

The type of coarse aggregate used was crushed stones of 80 - 150 mm from the viewpoint of the fluidity of the mortar in the caisson, availability, ease of handling, etc. The aggregate was stored at the rate of 200,000 m^3 maximum. It was then hauled to the site according to the construction schedule of each foundation. The most important task in the placing of the coarse aggregates was, ① to remove aggregates of grain size smaller than 80 mm, ② to remove fragments, silt, etc. that had adhered to the surface of the coarse aggregate. Therefore, the aggregate was not only passed through a drum scrubber, vibrating screen, etc. at the storage yard, but also a water curtain, vibrating screen, etc. on the barge at the foundation site, making an exhaustive effort to clean and screen the aggregate. Also, the water level in the caisson was raised to the top of the caisson to prevent aggregate from crushing.

4. Grouting of Mortar

(1) Material control

Table-2 shows the specified mix proportions. As the sea sand used was large in grain size, i.e. fineness modulus 2.5 - 3.5, it was adjusted to fineness modulus of 1.8 $\pm$0.2 in a rod mill. The sand was then stored in the storage yard, covered with a waterproof sheet and dried. The cement used was a fly ash cement made by pre-mixing ordinary Portland cement

with fly ash. Because the quality of fly ash differs depending on the power plant from which it is obtained, the quality of fly ash at each power plant was tested in advance for ignition loss, specific surface area, and carbon content, as well as confirming the shape by microscope, and then two power plants were selected for supply.

(2) Production of mortar

A mortar plant barge equipped with three mortar production plants, each of which has a production capacity of 2,000 ℓ/min., was used for mortar injection. Two plants were operated constantly, producing 4,000 ℓ/min. of mortar, the third one being used as a reserve. When producing mortar, the value of the mortar flow in the mixer was measured automatically for every batch, and the mortar within the range of 16.5±2 seconds was discharged to the agitator, with the rest being disposed of. The disposal ratio was about 0.3%. Also, the coefficient of the surface moisture of the sand was corrected by the average value of mortar flow. In addition, a sample was taken from the agitator for every 1,000 m^3 of production, and was tested in the laboratory on the plant barge.

(3) Mortar injection

The injection of mortar was performed continuously using 20 grouting pipes from the base to the top of the caisson. The mortar injection pipe was of a duplex type as shown in Fig-1, and the rise of mortar was automatically measured, according to which the pipe was raised. The rate of injection was 4,000 ℓ/min by using 20 pipes. The proportion for each pipe was determined according to the ratio of each injection area and the mortar flow was constantly measured and adjusted during the injection adhering to the dividing ratio. As a result, the level of the mortar was raised constantly and evenly.

5. Strength of Concrete

The concrete at the top of the foundation was removed to a depth of about 50 cm one month after the mortar injection. And the strength of concrete was measured throughout the entire area of the foundation using a schmidt hammer. Also, from two points, the points nearest to and farthest from the injection pipe, a large diameter core of 45 cm was taken throughout the total height of the foundation and compression tests were performed. The average compressive strength (age 91 day strength) of these was approximately 200 f/cm^2 for all foundations.

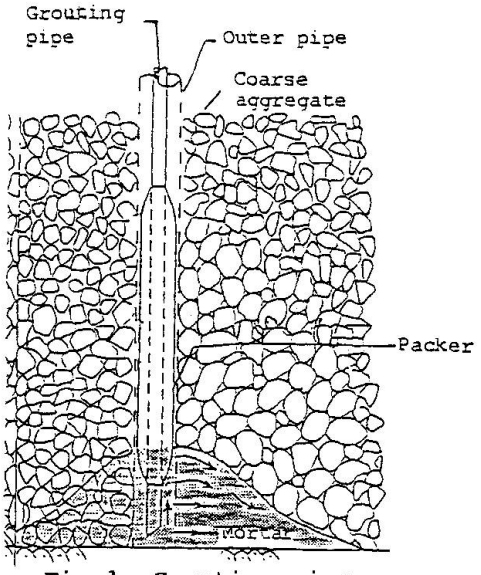

Fig-1 Grouting pipe

Table-1 Submarine Foundatin Major Factors

	Hitsugiishijima Bridge (HB)		Iwagurojima Bridge (IB)			Nanboku-Bisan-Seto Bridge (BB)						Total
	2P	3P	2P	3P	4P	2P	3P	4A	5P	6P	7A	
Plane dimension (m)	25 x 46	29 x 46	18 x 46	22 x 46	36 x 32	23 x 57	23 x 57	57 x 62	27 x 59	38 x 59	75 x 59	
Height of foundation base (TPm)	-28	-25	-15	-24	-14	-10	-10	-10	-32	-50	-50	
Top level of marine concrete	± 0	-12	± 0	± 0	- 2	± 0	± 0	± 0	± 0	+2.3	+2.3	
Solume of marine concrete	35,000	9,000	12,000	24,000	13,000	12,000	12,000	34,000	47,000	114,000	228,000	540,000

Table-2 Specified Mix Proportions

Coarse aggregate			Range of settling (sec)	Water-binder ratio W/(C + F) (%)	Admixture ratio F/(C + F) (%)	Sand-binder ratio S/(C + F)	Unit volume					
Minimum Size	Maximum size	Percentage of voids					W (kg)	C (kg)	F (kg)	S (kg)	Admixture (g)	Aluminum (g)
80	150	50	17±2	48	20	1	391	652	163	815	8,150	81.5

KOBE STEEL, LTD.

Design of Steel Pipe Grid Dam for Debris Flow Control

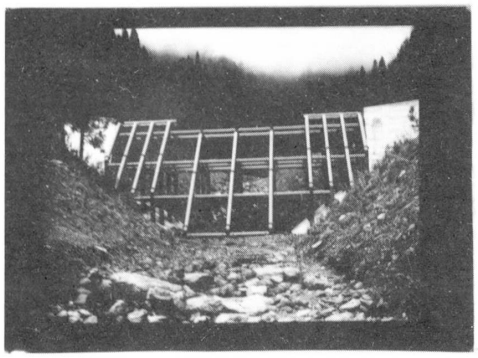

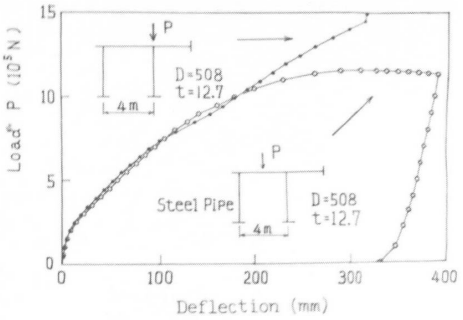

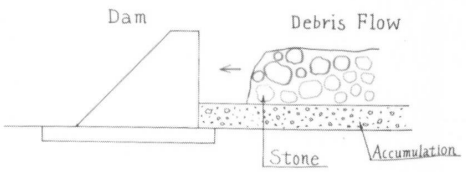

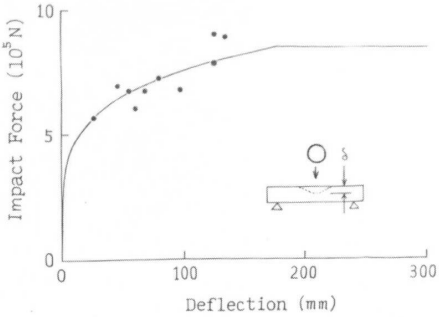

Design of Steel Pipe Grid Dam for Debris Flow Control

Hiroshi NAKANISHI
Kobe Steel, Ltd.
Kobe, Japan

Takahisa MIZUYAMA
Public Works Research Institute
Ministry of Construction
Tsukuba, Japan

Kazuyoshi NAKAJIMA
Kobe Steel, Ltd.
Kobe, Japan

1. DEBRIS FLOW CONTROL

Debris flow is one of the most serious types of natural desaster, and various studies on debris flow, on-site observation of debris flow, studies of prevention measures against the disaster and so on have been carried out up to this day. One of the countermeasures is prevention of occurence of debris flow in use of a group of small consolidation dams. And another countermeasure is control of the flowing condition of the debris flow in use of various types of dams.

A steel pipe grid dam is one of the control dams of the debris flow and consists of large-sized steel pipes latticed in a three-dimensional form, which aims at arresting hazardous running stones while at the same time adjusting the flow of sand and soil effectively.[1)]

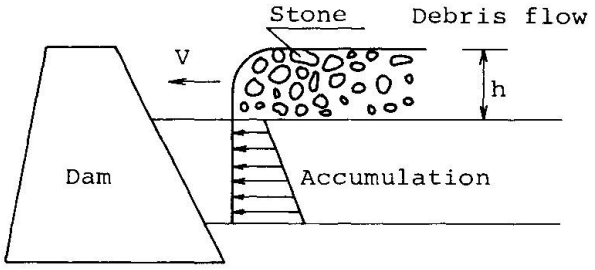

Fig.1 Debris flow

2. DESIGN OF STEEL PIPE GRID DAM

It is assumed that the dam is subjected to two kinds of loads which are stationary loads and impact forces.

(1) Soil pressure: Soil accumulates around the grid dam due to variation of a river bed, and the pressure acts on the grid dam.
(2) Fluid force: As if stones and gravels in the debris flow block up the grid of the dam, it is assumed that the fluid force of the debris flow acts on the dam all over.
(3) Inpact forces of stones: Huge stones are contained at the head of the debris flow as shown in Fig.1. The stones collide with the grid members of the dam and impact forces act on the member.

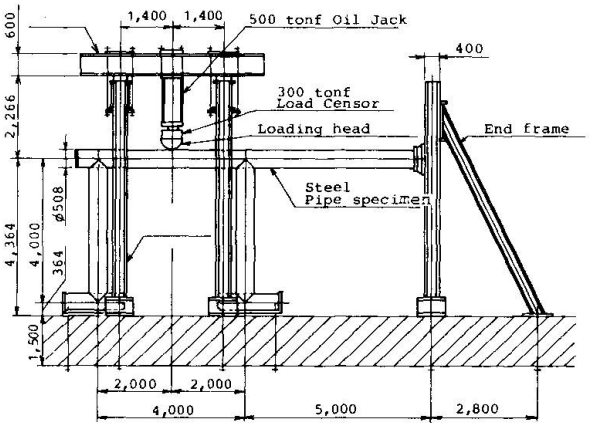

Fig.2 Loading test apparatus

The dam has to be stable against the soil and fluid pressures so as not to slide, roll over and collapse. While the dam has to be designed against the impact forces of stones so as not to lost the capacity of adjusting soil and sand discharge. It is considerably difficult to design it without a damage of the dam, because the more the dam is stiffened, the more the impact force increases. Therefore it is considered that the dam is allowed to have a local damage and that the kinematic energy of a stone is replaced to the strain energy of a grid member in inelastic deformation range.

3. CAPACITY OF ENERGY ABSORPTION OF A GRID MEMBER

Static loading tests of F-shaped frames consisting of steel pipes of 508mm in diameter and 12.7mm in thickness have been carried out as shown in Fig.2. The yield stress of the pipe material was 381MPa from results of a test, although the value of the Japanese standard about its material is 235MPa.

The load-deflection relation in case of loading at a midpoint of joints of pipes is shown in Fig.3 and the similar relation in case of loading at a joint is shown in Fig.4. The deflections of the test results in Fig.3 and 4 are shown as sums of the local denting deformation of the pipe wall and the overall bending deformation of the pipe.

The local dent has appeared at the initial state of loading, and at the following state of loading the overall bending and some additional local denting have yielded.

Analytical treatment of these local denting and overall bending damage has been reported in Ref.(2). From the report the relationship between the load and the dent depth has been given by

$$F_d = \frac{1}{4} K \delta_Y t^2 \left(\frac{\delta_d}{D}\right)^{1/2} \quad (1)$$

where δ_d : dent depth, D: diameter of a pipe, t: thickness of the pipe wall, δ_Y : yield stress of the pipe material, K: constant given by 150

The energy absorption, Ed, due to the dent is easily developed as

$$E_d = \frac{1}{6} K \delta_Y t^2 \left(\frac{\delta_d^3}{D}\right)^{1/2} \quad (2)$$

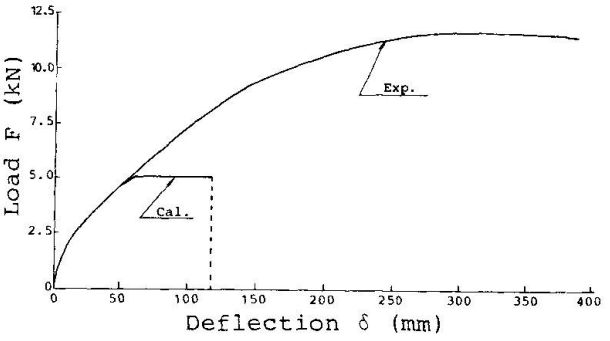

Fig.3 Load-deflection curve
Loading at the midpoint of joints

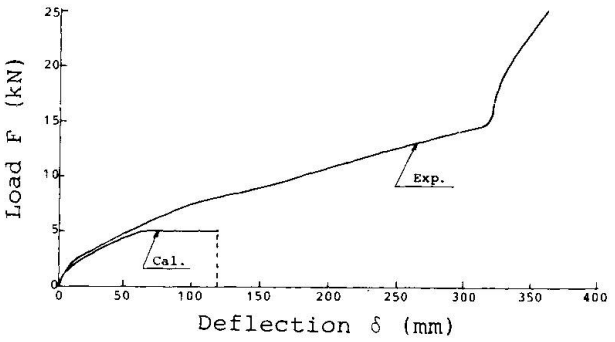

Fig.4 Load-deflection curve
Loading at a joint

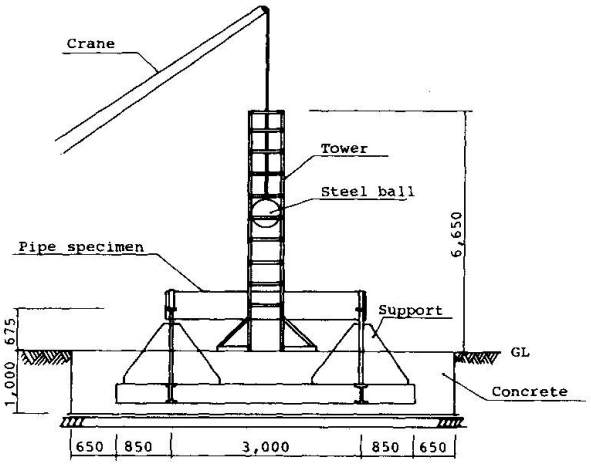

Fig.5 General view of impact tests

In addition, the overall bending collapse load, F_o, has been presented for the dented pipe fixed at the both ends as

$$F_o = \frac{4}{L}D^2 t\delta_Y(\cos\beta-\beta) \qquad \beta = \left(\frac{\delta_d}{D}\right)^{1/2}\left\{1 - \sqrt{\frac{16}{9}\left(\frac{\delta_d}{t}\right)^2 + 1} + \frac{4}{3}\frac{\delta_d}{t}\right\} \tag{3}$$

where L is a span length between both ends. The energy absorption, E_o, due to the collapse deformation is shown as

$$E_o = F_o\delta_o \tag{4}$$

where δ_o is the ultimate deformation at the loading point of the pipe. δ_d is obtained by solving simultaneously Eq.(1) and (3).

Substituting the yield stress on the Japanese standard into δ_Y in Eq.(1) and (3), a load-deflection relation of the tested pipe is obtained as a dotted line shown in Fig.3 and 4.

The ultimate deformation, δ_o, varies with a axial force, D/t and so on. In general, the member subjected to the lateral loading is in tension under the large lateral deformation, and the lateral load thereby does not decrease in its state.

For the pipe less than 40 in D/t, δ_o is assumed with enough safety as

$$\delta_o = 20\delta_E = 20\,\frac{L^2\delta_Y}{12ED} \tag{5}$$

where δ_E is the bending deformation at a midpoint of a pipe which give a yield stress to the surface fibre of the pipe. In case of the tested pipe

$$\delta_d = 60\text{mm}$$

and the quantity of the energy absorption of the test result is larger than 3 times as much as the estimated value.

4. IMPACT TESTS

A general view of impact tests is shown in Fig.5. The diameter and thickness of the pipe specimen are the same size as the pipe used in the static loading tests. The pipe were set on the both supports located 3m in distance. And a steel ball about 20kN in weight is lifted up 1m to 5m in height from a upper surface of the pipe, and fall down on the pipe.

Results of the tests are shown in Fig.6. In this test the magnitudes of the impact forces were in dent deformation range. A dotted line in Fig.6 shows a load-dent relation estimated by Eq.(1) in use of the yield stress in the Japanese standard. It is known that the estimated energy absorption is fairly less than the value of test results.

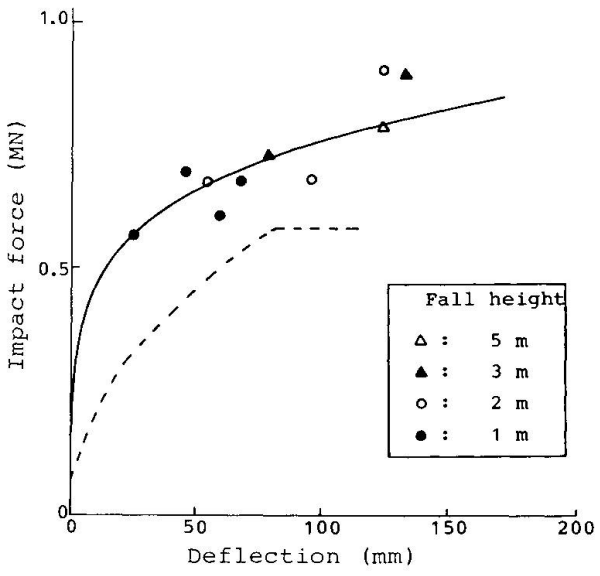

Fig.6 Impact force-deflection relation

Reference
(1) Namita, Y., korokuro-sawa Steel-pipe Grid Dam, Yamagata (Japan), IABSE STRUCTURES C-38/86, p58-59 IABSE PERIODICA, March 1986.
(2) Ellinas, C.P. and Walker, A.C.: Damage on Offshore Tublar Bracing Member, IABSE Colloquim, Ship Collision with Bridge and Offshore Structure, Copenhagen, 1983.

NAGOYA UNIVERSITY

S. Baba
K. Ninomiya
T. Kajita

Active Control of Bridge Structures Based on Modal Analysis

Concept of digital type active optimal control of suspension bridge is provided. One-to-one accurate control against an unsteady wind force caused by typhoon is realized by the use of step-by-step digital control, and it will possibly lead to a dual design, for which the bridge is designed only for the ordinary self-weight and traffic load, and for which the anti-wind capacity of the bridge is mainly supported by controlling.

State equation of 'equation of motion' under the action of control and external forces is described as follows in a continuous-time system:

$$\mathbf{A}\dot{\mathbf{X}}(t)+\mathbf{B}\mathbf{X}(t)=\mathbf{C}\mathbf{U}(t)+\mathbf{D}\mathbf{F}(t)$$

in which $\mathbf{X}^t=|\dot{x}_1,\cdots,\dot{x}_n,|\ x_1,\cdots,x_n|$ ($\mathbf{X}$: displacement), $\mathbf{U}$ is control force and $\mathbf{F}$ is external (wind) force. When the equation is represented in a discrete-time system, matrix exponential function appears and it gives a large defect on the numerical calculation. The efficiency of the iterative calculation is hugely improved by introducing an orthogonal technic based on the complex modal analysis into the state equation. Discrete type state equation is represented as follows:

$$\mathbf{x}(t+\triangle t)=\mathbf{B}^*\mathbf{x}(t)+\mathbf{C}^*\mathbf{U}(t)+\mathbf{D}^*\mathbf{F}(t)$$

Optimal value of control force $\mathbf{U}(t)$ is obtained, in a real time, based on the Pontrjagin's maximum principle. Let $\mathbf{U}(t)$ be positive (tensile only).

Suspension bridge is modelled as shown in Fig.1, in which girder of the bridge is discretized into isoparametric shell elements in order to represent a twisting motion, which will produce the most disadvantageous vibration mode to the suspension bridge. External forces used in the numerical examples are also shown in Fig.1. Deformation of the bridge is shown in Fig.2 and Fig.3, which correspond to the bending and twisting vibration, respectively. Thick lines implies the vertical displacements d_A and d_B (Fig.2) and torsional angles r_A and r_B (Fig.3) at points **A** (solid lines) and **B** (break lines). Thin solid lines (point **A**) and break lines (point **B**) imply the deformation without controlling. Control forces u_A and u_B in each case is indicated in the lower parts of Figs.2 and 3, in which right-side forces (u_A^2 and u_B^2) are shown by thin lines. Deformation d is non-dimensional value divided by the maximum deformation without controlling. Control state varies according to the selection of parameters specifying the balance between the allowable deformation and control capacity.

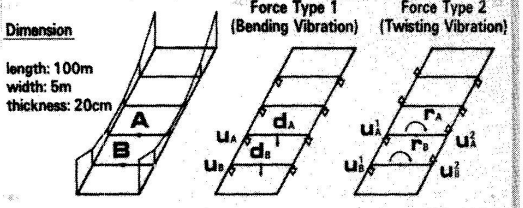

Fig.1 Suspension Bridge. ▽ external force

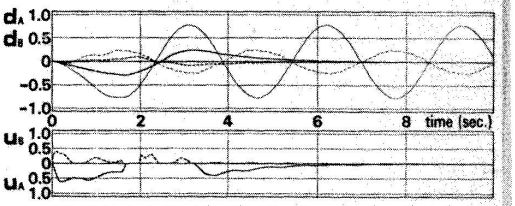

Fig.2 Control of Bending Vibration Caused by Force Type 1.

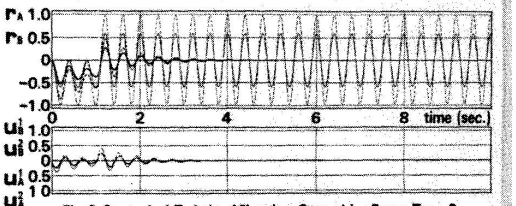

Fig.3 Control of Twisting Vibration Caused by Force Type 2.

Active Control of Bridge Structures Based on Modal Analysis

Shunsuke BABA
Dep. of Civil Engineering
Nagoya University
Chikusa, Nagoya, Japan

Kohki NINOMIYA
Dep. of Civil Engineering
Nagoya University
Chikusa, Nagoya, Japan

Tateo KAJITA
Dep. of Civil Engineering
Nagoya University
Chikusa, Nagoya, Japan

ABSTRACT

Digital type active optimal control of suspension bridge is provided. One-to-one accurate control against an unsteady wind force caused by typhoon is realized by the use of step-by-step digital control.

State equation represented in a digital form contains a matrix exponential function, and it gives a large defect on the calculation of control force. Efficiency of the calculation is hugely improved by using an orthogonal technic based on the complex modal analysis. Control of suspension bridge, for which the bending and twisting vibration is induced, is conducted as numerical example.

INTRODUCTION

Active optimal control, purposing to prevent a structural vibration, has been applied to the civil engineering field in the 1970's by Abdel-Rohman, Carotti, Leipholz, Lin, Yahagi and Yang. However, in those cases, the state equation has been formulated in the analogue type control system. The system is inappropriate to one-to-one accurate control, which is the most reliable control method against an unsteady state. They have restricted the problem in a steady state as a regulator problem, or they have re-formed the problem into a quasi-steady state using the frequency response functions.

The writers have worked on the digital type control[1]. The digital control is realized by calculating the optimal control forces, step-by-step, against the unsteady external forces. The advantageous point of the system is the one-to-one correspondence between external and control forces. The disadvantageous point is the numerical calculation which needs a high-speed, large-capacity computer[1], and it can be improved by the use of complex modal analysis. The digital control, therefore, can be applied practically to the control of the multi-nodes consistent-mass structure.

The digital control is applied not only as a supplementary tool to decrease an unpleasant vibration, but also as a principal mechanism to prevent a structural collapse due to strong wind. The digital control of suspension bridge is provided as numerical example, where isoparametric shell element is employed.

OBSERVATION AND CONTROL

The following two assumptions are used:

1. Magnitude of the future wind force is assumed as zero. It implies only the present value of wind force is reflected on the control.

2. Present state of the structural deformation is substituted by the simulative value obtained numerically by solving the equation of motion.

STATE EQUATION

Equation of motion under the action of control force $\mathbf{u}(t)$ and wind force $\mathbf{f}(t)$ is represented as follows, if the viscous damping is ignored:

$$\mathbf{M}\ddot{x}(t) + \mathbf{K}x(t) = \mathbf{u}(t) + \mathbf{f}(t) \qquad (1a)$$

in which $x(t)$ is a nodal displacement vector, $\mathbf{K}$ is a stiffness matrix and $\mathbf{M}$ is a consistent mass matrix. The second order differential equation in Eq.(1a) is modified to a form of equation of evolution, for which the Pontrjagin's maximum principle is applicable, by introducing the following two relations:

$$\mathbf{M}\dot{x}(t) - \mathbf{M}\dot{x}(t) = \mathbf{0} \qquad (1b)$$

$$X(t)^{T} = \{\dot{x}_1(t) \cdots \dot{x}_n(t) \mid x_1(t) \cdots x_n(t)\} \qquad (2)$$

in which $\mathbf{X}(t)$ is a state variable vector. State equation of control is expressed as shown in the first equation in our poster; that is,

$$A\dot{X}(t) + BX(t) = CU(t) + DF(t) \qquad (3)$$

$$A = \begin{bmatrix} 0 & M \\ M & 0 \end{bmatrix} \quad B = \begin{bmatrix} -M & 0 \\ 0 & K \end{bmatrix} \quad C = \begin{bmatrix} 0 \\ I_u \end{bmatrix} \quad D = \begin{bmatrix} 0 \\ I_f \end{bmatrix}$$

In whixh $\mathbf{I}_u$ and $\mathbf{I}_f$ are transformation matrices which represent the direction of control and wind forces, respectively.

Let the nodal displacement x be expressed as

$$x(t) = \phi \exp(\omega t)$$

and therefore $\mathbf{X}(t)$ can be represented as the product of eigen matrix Φ ($\Phi^{T} = [\phi\omega \mid \phi]^{T}$) and generalized displacement vector $\mathbf{Q}(t)$ as follows:

$$\mathbf{X}(t) = \Phi\,\mathbf{Q}(t) \qquad (4)$$

in which ϕ is an eigen vector, ω is a diagonalized eigen value matrix.

The state equation Eq.(3) is represented in the followings [the second equation in our poster] by introducing Eq.(4) and by assuming the 0th order hold, where let $\mathbf{U}(t)$ and $\mathbf{F}(t)$ be constant during the time interval Δt:

$$x(t+\Delta t) = \mathbf{B}^{*}x(t) + \mathbf{C}^{*}U(t) + \mathbf{D}^{*}F(t) \qquad (5)$$

$$\mathbf{B}^{*} = \phi A(\phi^{T}\phi)^{-1}\phi^{T}, \quad \mathbf{C}^{*} = \phi B \phi^{T} I_u, \quad \mathbf{D}^{*} = \phi B \phi^{T} I_f$$
$$A = \exp(\omega \Delta t), \quad \mathbf{B} = -(2\omega\phi^{T}M\phi)^{-1}[I - \exp(\omega\Delta t)]$$

OPTIMIZATION

Hamiltonian H is defined as follows:

$$\begin{aligned} H = {} & (1/2)[x^{T}(t+\Delta t)Rx(t+\Delta t) + x^{T}(t+2\Delta t)Rx(t+2\Delta t)] \\ & + (1/2)[U^{T}(t\ \ )SU(t\ \ ) + U^{T}(t+\Delta t)SU(t+\Delta t)] \\ & + \lambda^{T}(t+\Delta t)[-x(t+\Delta t) + B^{*}x(t\ \ ) + C^{*}U(t\ \ )] \\ & + \lambda^{T}(t+2\Delta t)[-x(t+2\Delta t) + B^{*}x(t+\Delta t) + C^{*}U(t+\Delta t)] \end{aligned} \qquad (6)$$

In which λ is a Lagrangean multiplier vector, $\mathbf{R}$ and $\mathbf{S}$ are weight matrices defined in diagonal forms as ($\mathbf{I}$: unit matrix)

$$\mathbf{R} = \alpha \mathbf{I} \quad , \quad \mathbf{S} = \beta \mathbf{I} .$$

Rate of α to β, α/β, is an important scalar index in the control problem; that is, if the ratio α/β is selected as small value, control force will be small and the control effect becomes also small, on the contrary if the ratio is large, strong control effect is expected.

Conditions for the optimization are as follows:

$$\begin{aligned} \partial H/\partial x(t+\Delta t) &= 0 \quad , \quad \partial H/\partial x(t+2\Delta t) = 0 \quad , \\ \partial H/\partial U(t\ \ ) &= 0 \end{aligned} \tag{7}$$

NUMERICAL EXAMPLE

Digital control of suspension bridge, as shown in Fig.1, is provided. Control forces $U(t)$ are applied to the structure as vertical pull forces generated by hydraulic power of the tendons, which is attached in parallel with vertical hanger cables. Compressive forces cannot be generated by the tendons, henceforth the following constraint is introduced in the numerical analysis:

$$U(t) \geq 0 \tag{8}$$

Let the vertical external force $P = 1$ be applied suddenly, at the time $t = 0$, to the equally divided five points as shown by arrow symbols in Fig.1, and let it be removed at $t = 1.56$ second (Force type 1) and $t = 1.00$ second (Force type 2). Force type 1 corresponds the bending vibration, and force type 2 is twisting vibration. Time interval Δt is selected as 0.02 second.

In the case of bending vibration [see Fig.2], vertical displacements at the points A and B of slab, indicated by d_A and d_B, are shown by a thick solid line and thick break line, respectively. Displacements are represented in non-dimensional quantities divided by the maximum displacement in the un-controlled case, which is shown by thin lines as a comparison. Control forces are also shown in Fig.2, in which forces u_A and u_B are shown by solid and break lines, respectively. The ratio α/β is selected as 10^{-3}.

In the case of twisting vibration [see Fig.3], axial rotation angles at the points A and B, indicated by r_A and r_B, are shown by a thick solid line and thick break line, respectively. Rotation angles are represented in non-dimensional quantities based on the un-controlled case, which is shown by thin lines. Control forces are also shown in Fig.3, in which forces u^1_A, u^1_B (left side) and u^2_A, u^2_B (right side) are shown by solid and break (A: thick, B: thin), respectively. The ratio α/β is selected as 10^{-4}.

CONCLUSION

Active optimal control in discrete-time system, diagonalized based on the complex modal analysis, becomes an efficient tool in the control problem of the suspension bridge under wind motion.

REFERENCES

1. Baba, S., Ninomiya, K., Kajita, T., Servo-strengthening system in large-scale suspension bridge, Proc. 13th IASTED Int. Conf. on Modelling and Simulation, Lugano, 1985, 341.

HANSHIN
EXPRESSWAY
PUBLIC CORPORATION

H. TOTTORI

Vehicle's Axial Weight Measuring Apparatus

1. Introduction

The Hanshin Expressway Public Corporation installs a vehicle's axial load measuring apparatus (a platform scale) at each tollgate and tollbooth. The introduction of the apparatus helps detect violations of vehicls' weight, which means prevention of damage to the road, and therefore contributes to the safe traveling of the vehicles.

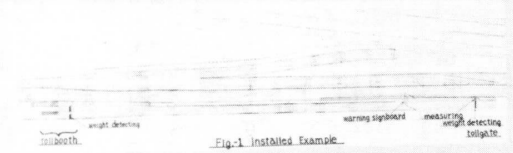

Fig.-1 installed Example

Fig.-1 shows part of the Hanshin Expressway (Wangan Route, near Dejima tollgate, which is under construction), where a platform scale is installed.

Fig.-2 illustrates the standard system of a platform scale, which consists of the following five functional sections:

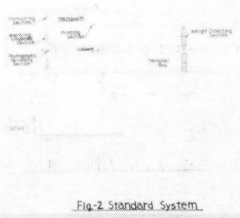

Fig.-2 Standard System

(1) weight detecting section

The weight detective section is buried in the pavement at the same level of the road surface. When vehicles move over this part, it finds their axial load, and the detected weight is transformed into an electric signal. The loading plate (the detecting part) is 760 mm in width and 1,600 mm in length and two plates are used per traffic lane (3,200 mm). It's thickness gauges 70 mm and 180 mm, one of which is used for overpass roads and, the other for ordinary roads. A loadcell is used for the converter, and when it is thin, twelve loadcells are used and when it is thick, eight.

(2) measuring section;

This is the control center of the scale, where the electric signal from the detecting section is turned into the weight value. This section judges whether the weight exceeds the limited figure or not, and thus is the core of the system sending various signals to other sections of the apparatus. The outer size of this section is 570 mm wide, 710 mm deep, and 1,000 mm (including the length of the caster) high.

(3) printing section in the booth;

On receving the signal from the measuring section indicating that the measured weight figure exceeds the limitation set by the Vehicle Limitation Law, this section publishes a warning sheet, in which the weight figure and the date are printed. The warning sheet is handed to the driver of the vehicle. The outer size of this section is 250 mm in width, 335 mm in depth, and 340 mm in height.

(4) warning signboad section;

The driver is warned by both the warning sheet explained above and the electric signboad which shows the violating weight figure. The outer size of the signboad is 1,600 mm wide, 500 mm deep, and 650 mm high.

(5) photographic recording section;

If the weight figure exceeds the limitation, the measuring section (control center) directs this section to take photographs of the vehicle's license plate number, the driver, and the car body. At the same time, the date, the vehicle's axial weight, and the name of the measuring place are recorded on the same photographs taken here. The outer size of this part is 315 mm × 295 mm × 560 mm.

Leere Seite
Blank page
Page vide

NIHON DORO KODAN

JAPAN
HIGHWAY
PUBLIC
CORPORATION

QUALITY ASSURANCE OF BRIDGE CONSTRUCTION WORKS AT NIHON DORO KODAN

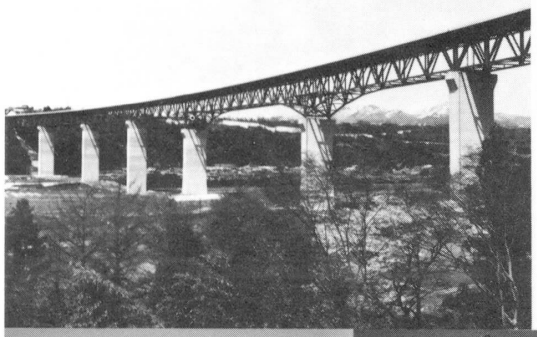

KATASHINA-RIVER BRIDGE

◀1.

Bridge length : 1033.85m
Span : (74.5 + 104.3 + 83.5) + (116.9 + 168.85 + 116.9) + (116.9 + 130.0 + 116.9)m
Width : 20.0m
Girder depth : 14.0m
Steel weight of superstructure : 9963t

CANTILEVER ERECTION BY TRAVELLING CRANE 2. ▶

Superstructure was erected by travelling crane cantilever method from both abutments. In order to absorb elastic and temperatural deflections during erection, temporary pedestal frames with sliding surface were employed on piers.

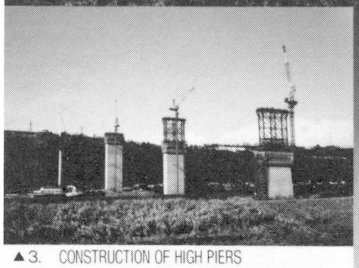

▲3. CONSTRUCTION OF HIGH PIERS

High piers were constructed by tower cranes and self-climbing forms. The highest pier is 69.4m. Seismic shaking test was conducted after the completion of piers.

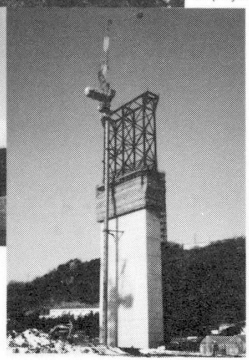

◀4. INSTALLATION OF STEEL

Reinforcing steel block was installed by tower crane. Both steel and bars were used as reinforcement of piers in order to assure ultimate strength and execution efficiency.

AUTOMATIC GAS-PRESSURE WELDING 5. ▶

Automatic gas-pressure welding for reinforcing bars was employed in order to assure quality and execution efficiency. Ultrasonic inspection was used to test the quality of the joints.

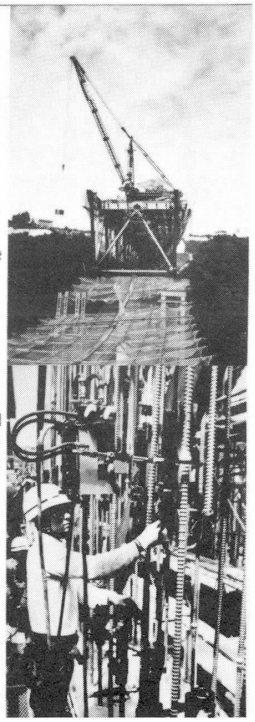

Quality Assurance of Bridge Construction Works at Nihon Doro Kodan

Eiji NAKASHIMA
Head of Struct. Eng. Sect.
Nihon Doro Kodan
Tokyo, Japan

Michiaki SAKATE
Deputy Head of Struct. Eng. Sect.
Nihon Doro Kodan
Tokyo, Japan

1. Introduction

Nihon Doro Kodan (Japan Highway Public Corporation) has constructed about 3,700km length of expressways all over Japan until now and been operating the constructed expressways. Moreover, it is constructing or surveying about 2,000km length expressways at present.

As more than 70% of Japanese land is mountaneous, high technology is required in bridge construction. High piered bridges of the Kan'etu Expressway , which were granted Tanaka Award (Award for Bridges) of 1985 from Japan Society of Civil Engineering, are a good example of this. The bridges were constructed over various technical difficulties.

In this paper, we will introduce concept and method of Nihon Doro Kodan's bridge quality assurance as an owner when the construction works are contracted.

2. Standard for quality assurance

Nihon Doro Kodan specifies the following quality standards and mannuals for quality control relating to bridge construction works.

(Material and Construction)

a. Test Mannual for Construction Control

b. Standards of Material Application

c. Painting Standards for Steel Bridges

d. Execution Instruction for Arc Stud Dowel Welding

e. Standards for Expansion Joint of Bridges

f. Standards for Non-Shrink Mortar

(Supervising and Inspection)

a. Mannual for Supervising

b. Inspection Standards for Structures

All of these standards are meant for practical execution of contents which are stated in the contract document, the standard specification and the design mannual.

3. Methods for quality assurance

The difficulty of bridge construction works is that it is not easy to reform the completed structures. It is crucial to decide clearly how far the owner attend and inspect during construction, how far the owner submit the quality control to the contracter, namely, the roles of the two. Moreover, the roles should be reconsidered as time passes.

The current basic concept of Nihon Doro Kodan for quality assurance is that the assurance should be achieved through the approval, direction, attendance, test and inspection by the owner.

Materials used in our bridge construction are generally those which are standardized by Japanese Industrial Standards, but for non-standardized materials, Nihon Doro Kodan specifies its own quality standards. In such a case, material tests are carried out under the attendance of the owner.

Construction work is executed after the approval of the execution plan which is submitted by the contracter. In all stages of the construction work, Nihon Doro Kodan gives necessary directions to the contracter. Daily and

periodic quality control tests specified by Nihon Doro Kodan are carried out on the contracter's responsibility and, if necessary, they are attended by the owner.

4. An example of quality assurance

The three bridges of Katashina-river, Nagaigawa-river and Numao-river have the largest scale among bridges which have been built in mountaneous areas of Japan.

Therefore, from the planning stage, an committee on their design and construction was established and various analysises were executed mainly as to their structure type and aseismicity for three years.

As a result, steel reinforced concrete hollow flexible structures with box-sections were adopted for high piers. Two metal bridges, Katashina-river and Numao-river, were decided to be types with multi-fixed support on high piers in order to assure aseismicity. On the contrary, Nagai-river bridge adopted elastomeric bearings which transmit seismic horizontal force of 4,000 ton to an abutment.

Based upon the recommendation of the committee, various dynamic analysises and shaking tests of 1/100 scale model, a completed pier and the whole structure were executed in order to verify the the design procedure.

On the construction side, automatic ascending forms with scaffoldings were newly developed. Placement of concrete more than 80m high above the ground level, which had not been achieved before, was done by specially modified concrete pumps. Moreover, for numerous large-diameter reinforcing bar joints, new methods such as automatic gas welding were developed.

In the case of Numao-river bridge, the whole girder of 600m was continuously erected by lauching girder with computer-aided center control system and after that the entire girder of 3,000 ton was transformed transverselly. This method was adopted due to the height of the erection site and lack of the space.

KAWADA INDUSTRIES, INC.

DENKA

NEW APPLICATION OF POLYMER CONCRETE IN REHABILITATION OF EXPANSION JOINT

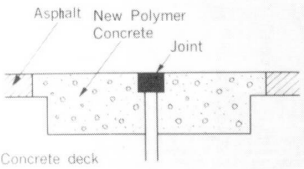

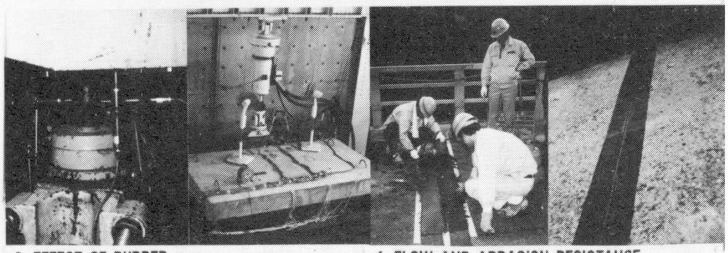

1. BACKGROUND

The main cause of damage of end dam concrete is considered as large repeated impact of vehicles due to the different lebel between the end dam concrete and expansion steel or asphalt.

Therefore, We consider that excellent impact resistance and abrasion resistance of end dam concrete must be the most important characteristics and developed resin concrete, which is mixture of convensional epoxy resin and synthetic rubber.

2. FEATURES OF NEW CONCRETE

This concrete has a low coefficient of elastisity ($E = 2 \sim 8 \times 10^4$kg cm^2)and is applicable to low temperature.

The component materials are as follows ;

Binder : mixture of epoxy resin and chloroprene rubber.

Aggregate : dry sand and crushed stone.

3. EFFECT OF RUBBER

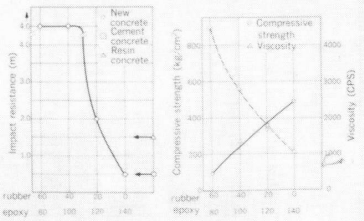

FIG.1 IMPACT RESISTANCE AND RUBBER WEIGHT

FIG.2 COMPRESSIVE STRENGH AND RUBBER WEIGHT

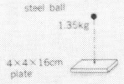

Impact strength test

The mixture ratio of the epoxy resin and the rubber gives an influence on the dynamic characteristics, the time of hardening and the workability.

4. FLOW AND ABRASION RESISTANCE

Type	New concrete	Resin concrete	Cement concrete
New material binder	1		(kg)
Resin concrete binder		1	
cement			400
Fine aggregate	3	3	650
Coarse aggregate	5	5	1,240
Water			150
Flow resistance	0.01mm	0.01mm	
Abrasion resistance(cm²)	0.04	0.34	1.65

Flow resistance : Wheel tracking test

Tire contact pressure	6.4kg cm^2
Temperature	60°C
Testing time	60min.

Abrasion resistance : Ravelling test

Chain	7mm dia. cross-chain
Temperature	−10°C
Testing time	90min.

New Application of Polymer Concrete in Rehabilitation of Expansion Joints

Shoji MIYAZAKI
Kawada Industries, Inc.
Tokyo, Japan

Shohei IKI
Kawada Industries, Inc.
Tokyo, Japan

Yukie NODA
Kawada Industries, Inc.
Tokyo, Japan

1. PREFACE

In order to reopen the road to traffic immediately or in at least a few hours after repair of an expansion joint, high-early-strength concrete or resin concrete are widely used on the end dam to fill the gap between the new expansion joint and concrete slab or pavement. But the difference in coefficient of thermal expansion between normal and resin concrete lead to early cracks and finally to destruction of the resin concrete dam and further more, the end dam concrete must take a repeated impact force from the traffic.
To cope with this phenomenon, resin concrete should be given a cohesive and elastic characteristic to be able to dissipate the stress caused by the difference in coefficients of thermal expansion. This characteristic will prevent the cracking as well as improve the resistance to impact and abrasion of the resin concrete.
To fulfill these requirements a new resin concrete (elastomeric concrete) has been developped by adding synthetic rubber to ordinary epoxy resin concrete. This material has a relatively low coefficient of elasticity compared to conventional resin concrete.

2. MATERIALS USED

The components of elastomeric concrete are as follows.
- Binder: Mixture of epoxy resin and liquid chloroprene rubber.
- Fine Aggregate: Dry sand (No.7 + No.4).
- Coarse Aggregate: Dry crushed rock

3. CHARACTERISTICS OF ELASTOMERIC CONCRETE

The ratio of mixing the epoxy resin with rubber is an important factor which will influence not only the dynamic characteristics, but the required time for hardening and its workability.
The hardening time normally depends upon the atomospheric temperature during placement and curing of the concrete and it is possible to reduce the time for the concrete to harden with a high curing temperature.

(1) THE EFFECT OF RUBBER

From test results, it can be recognized that the impact resistivity increases in proportion with the increase of the rubber component and an extremely big change can be observed between the ratio of rubber and epoxy (rubber/ epoxy) of 0.4 and 0.25.
The compressive strength decreases in proportion with to the rubber content, but the viscosity of the binder becomes higher as the weight of rubber increase, therefore the workability goes down.
In addition to the strength, the resin to rubber ratio of 0.4 provides a low viscosity as well as a favorable workability.

(2) RESISTANCE TO ABRASION AND FLOW

A wheel tracking test and a ravelling test were performed under conventional methods (see poster).
Table-1 illustrates the results of the comparison test among the ultra-high-early-strength cement concrete, normal resin concrete and elastomeric concrete.
In the flow resistance test, there was no flow and showed no difference due to the type of material.
However, in respect to abrasion resistivity, the elastomeric concrete showed excellent characteristics.
These results show that the effects of rubber in the elastomeric concrete are recognizable.

(3) VISCOSITY AND WORKABILITY

The workability is affected by the viscosity of the binder and this viscosity is highly affected by the temperature.
When the viscosity of elastomeric concrete becomes lower than 2000 cps, the slump will be 5 to 6 cm. Therefore, good workability can be obtained.
Fig. 1 shows the relationship between the viscosity of binder and temperature.
The results indicate that a minimum temperature of 15°C is necessary in order to maintain favorable workability.
As a result, it is recommended to heat the binder and the hardener at worksite in winter.

(4) INITIAL HEATING CONDITIONS AND STRENGTH

Fig. 2 indicates the curve showing the relationship of compressive strength with time.
In this test, the test piece of elastomeric concrete is cured for an hour under the condition of a constant hot curing temperature, then it is left to cool under atmospheric temperature.

The result of the experiment shows that when atmospheric temperature is below 10°C, it is not possible for the elastomeric concrete to harden in a short time.
During the hardening process, elastomeric concrete generates much heat. By this heat the hardening time can be considerably accelerated.
Therefore, it is necessary for the concrete temperature to reach the temperature of reaction as early as possible.
In winter a curing temperature of 50°C to 60°C is thought to be necessary.

4. SUMMARY

- When the components of rubber in the Binder increase, the impact resistance of the elastic concrete also increases but the workability and the hardening time will decrease.
- The inclusion of ruber in the Binder gives a considerable improvement in the abrasion resistance.
- It is necessary to maintain the temperature of the Binder in order to keep a favorable workability in winter.

Table-1

Type	New concrete	Resin concrete	Cement concrete
New material binder	1		(kg)
Resin concrete binder		1	
cement			400
Fine aggregate	3	3	650
Coarse aggregate	3	5	1,240
Water			150
Flow resistance	0.01mm	0.01mm	--
Abrasion resistance(cm^2)	0.04	0.34	1.65

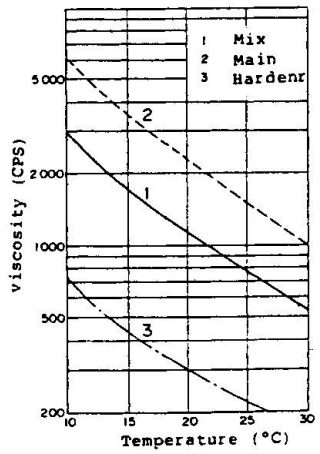

FIG. 1

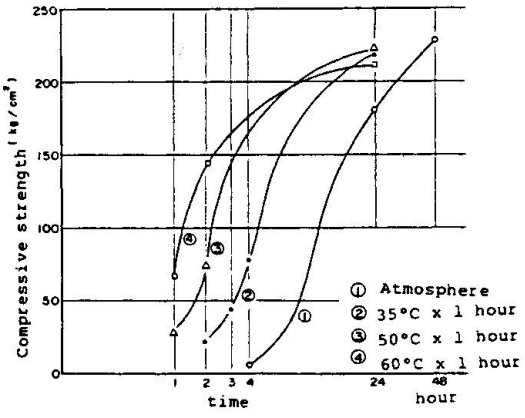

FIG. 2

NIHON DORO KODAN

JAPAN
HIGHWAY
PUBLIC
CORPORATION

APPLICATION OF EXPANSIVE CONCRETE TO REINFORCED CONCRETE DECK SLAB

BRIDGES APPLIED OF EXPANSIVE CONCRETE

No.	NAME OF BR.	CROSS SECTION TYPE	THICKNESS OF DECK SLAB (cm)	DESIGN STRENGTH OF CONCRETE (kgf/cm^2)	SPECIFIED MIX (kgf/m^3)				MAXIMUM AMOUNT OF EXPANSION OF REINFORCED CONCRETE DECK SLAB ($\times 10^{-6}$)		
					$\frac{w}{c+e}$ (%)	WATER CONTENT w	CEMENT CONTENT c	CONTENT OF EXPANSIVE AGENT e	AMOUNT OF EXPANSION TESTED BY JIS A 6202	TRANSVERSE DIRECTION	LONGITUDINAL DIRECTION
1	KUROISHIHAMA BR.	①	24	300	41.2	160	345	35	320	267	190
			24	300	41.2	160	380	—	—	—	—
2	TARAMI BR.	②	21	240	50.3	161	285	35	253	215	156
			21	240	50.3	161	320	—	—	—	—
3	KOSUGE BR.	①	24	240	47.0	141	265	35	257	163	123
			24	240	47.0	141	300	—	—	—	—
		③	24	240	47.0	141	265	35	303	49	70
			24	240	47.0	141	300	—	—	—	—
4	KURINOKI-RIVER BR.	④	23	240	56.4	172	260	45	425	240	200
			23	240	57.3	172	300	—	—	—	—
5	MARUKI BR.	①	23	240	54.7	164	265	35	220	143	88
			23	240	54.0	162	300	—	—	—	—

Upper side; Reinforced concrete with expansive agent
Lower side; Reinforced concrete without expansive agent

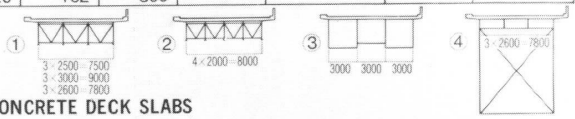

CRACKING ON BOTTOM SURFACE OF REINFORCED CONCRETE DECK SLABS

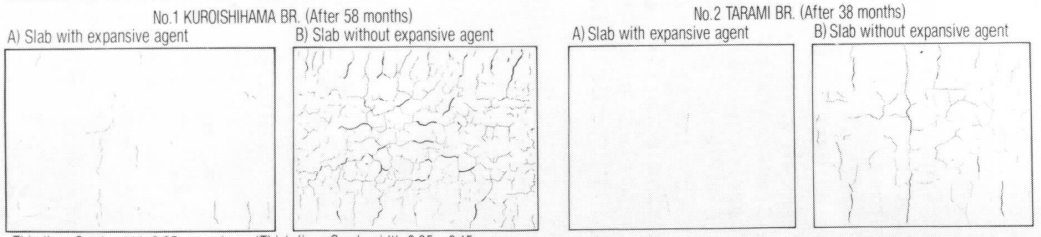

Thin line; Crack width 0.05mm or less / Thick line; Crack width 0.05 – 0.15mm

Application of Expansive Concrete to Reinforced Concrete Deck Slab

T. TOYOFUKU
Nihon Doro Kodan
Tokyo, Japan

T. META
Nihon Doro Kodan
Tokyo, Japan

Y. INOKUMA
Nihon Doro Kodan
Tokyo, Japan

1. Introduction

The deterioration process of reinforced concrete deck slab in steel road bridge can be explained as follows, according to loading test and survey on the existing bridges by Nihon Doro Kodan.

(1) Initial cracking due to drying shrinkage,subsidence, thermal stress and all that.
(2) Crack extention from top to bottom surface due to drying shrinkage
(3) Rain water infiltration into cracking zone.
(4) Abrasive action between crack surface by cyclic wheel loading and accelerating abrasion due to existence of water.
(5) Decrease of shear capacity.

Therefore, it is effective for the increase of durability of reinforced concrete deck slab to prevent initial cracking. Nihon Doro Kodan has applied experimentally expansive concrete to reinforced concrete deck slab of steel bridges shown in Table-1 since 1980 in order to cope with initial cracking.
Prior to the application, testing was conducted to know the influence of kinds and quantity of expansive agent on amount of expansion and compressive strength of concrete. And the observation is being made to know the difference of cracking behavior, temperature, strain variation caused by bridge types and meteorological condition.

2.Mixing

The specified mix is shown in Table. In case of expansive concrete, 35 kg/m of cement content in normal concrete was replaced by expansive agent, for it was found out by testing that the same compressive strength as normal concrete is obtained by the replacement while amount of expansion increase in proportion to content of expansive agent. But,the compressive strength of concrete tends to decrease when content of expansive agent exceeds 35 kg/m^3. The reason why expansive agent of 45 kg/m^3 was replaced in Kurinoki-River bridge was not only to reduce initial cracking, but to induce higher chemical prestress to concrete. And cement content of 5 kg/m^3 was added to compensate the decrease of compressive strength of concrete.

Table-1 Bridge Type

Name of Bridge	Type of Bridge	Bridge Length (m)	Compressive Strength of Concrete at the age of 28 days (kgf/cm^2)
Kuroishihama Bridge	Simple Composite Steel Plate Girder	41.5	446 384
Tarami Bridge	4-span Continuous Non-Composite Steel Plate Girder	149.2	331 335
Kosuge Bridge	2-span Continuous Non-Composite Steel Plate Girder	46.5	343 310
	3-span Continuous Non-Composite Steel Box Girder	157.0	344 344
Kurinoki-River Bridge	3-span Continuous Steel Truss	265.7	312 310
Maruki Bridge	4-span Continuous Non-Composite Steel Plate Girder	170.0	281 317

Upper Side : Expansive Concrete
Lower Side : Normal Concrete

3. Expansion

Amount of expansion shown in Table is the elongation of reinforcing steel bars in reinforced concrete deck slabs. Amount of expansion in transverse direction are larger than that in longitudinal direction. As the box girder bridge has higher flexual stiffness compared with that of other bridges, amount of expansion of box girder in Kosuge bridge is smaller than that of other bridges.

It was clalified that amount of expansion differs by the direction and the type of of bridges.

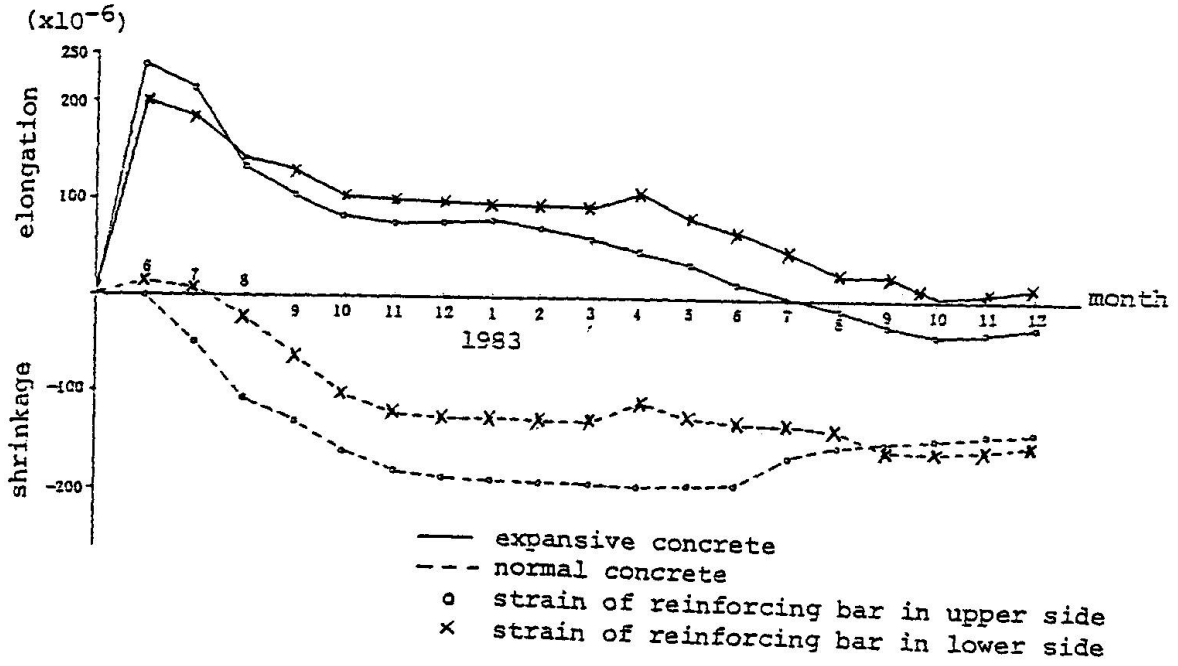

Fig-1 Time-dependent strain variation of reinforcing bar of deck slab in transverse direction.

4. Cracking

As shown in Table which describes the cracking on bottom surface of deck slabs of Kuroishihama and Tarami bridge, cracking in case of expansive concrete is remarkably little in comparison with that of normal concrete. This phenomenon was observed in other bridges as well.

Fig-1 shows the time-dependent strain variation of reinforcing steel bars in normal and expansive concrete deck slab of Tarami bridge.

In case of expansive concrete, maximum amount of expansion was 250×10^{-6}, but expansion was compensated by drying shrinkage of concrete after ayear. On the other hand, in case of normal concrete, drying shrinkage of 200×10^{-6} occurs and tends to crack. The difference of cracking between normal and expansive concrete can be proved by this time-dependent strain variation.

It was confirmed that a good effect in prevention of initial cracking by use of expansive concrete can be expected.

ADDITIONAL PRE-STRESSING FOR REPAIR STRENGTHENING PURPOSES

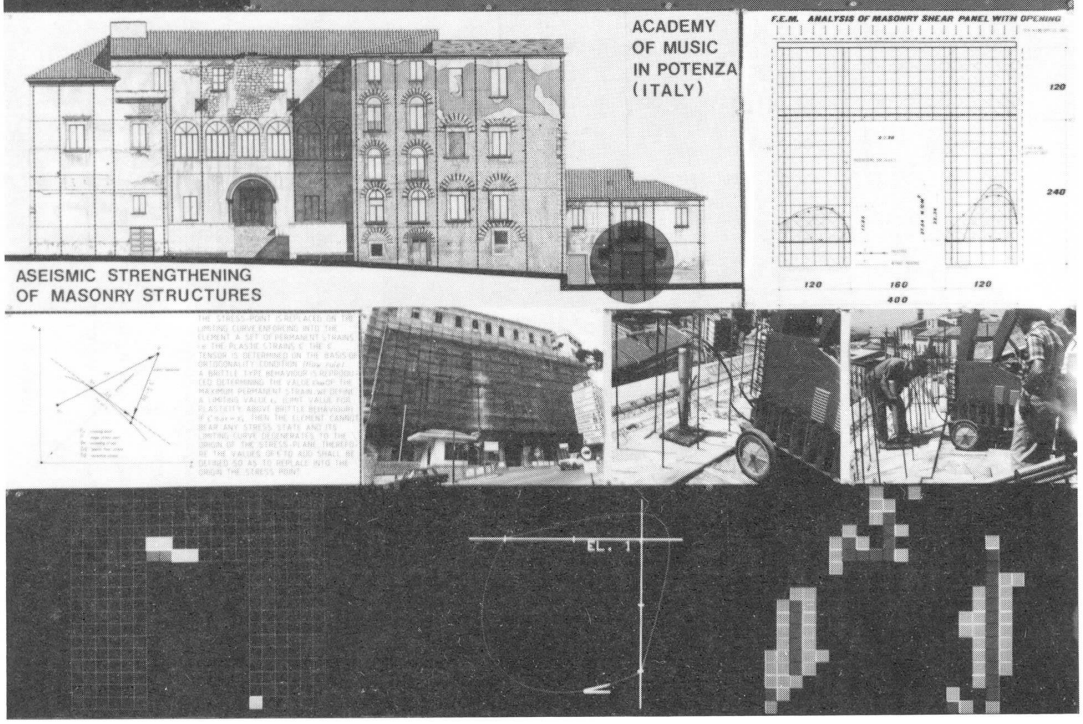

Additional Pre-Stressing for Repairing and Strengthening Purposes

N. AVRAMIDOU
Prof.
Fac. Archit, Univ. Firenze
Firenze, Italy

R. SPARACIO
Prof.
Fac. Eng., Univ. Napoli
Napoli, Italy

A design criterion for repairing damaged masonry buildings, in order to attain a desired safety level, must give schemes as "box-type" or "folded structures". For this purpose,effective connections between orthogonal walls are obviously required,as well as tie-beams running through wall elements at all floor levels,in order to get slabs infinitely rigid in their own plane. Such a criteria allow to evaluate the safety factor by analysing just the vertical walls,to determine the plane-stress distribution under monotonically increasing shearing forces and constant vertical load. Such a non-linear analysis,useful for seismic design,has been performed via computer program "N.IN.F.E.A." [1]; a two-dimensional plane-stress finit element has been used to model masonry panel,and beam element or road element for tie-beam and concentrated reinforcement. This way it is possible to evaluate the seismic behaviour of walls provided of pre-stressed steel cables as in the project ilustrated in this poster. The stress state is defined in a bi-dimensional continuum membrane loaded by forces acting in the middle plane of panel. The membrane may have holes with openings, as in the case of masonry panel of buildings.

The unknowns of the problem are the nodal generalized displacements; the equations are the equilibrium conditions for the nodal points under the actions of external and internal forces. These forces are related to elemental deformation and therefore they are expressed in terms of unknown displacements.

The numerical procedure is a typical step-by-step incremental loading analysis; for each element of the assemblage the elastic compatibility has been checked in every step. This means that the representative stress-point $P(\sigma_1,\sigma_2)$ is contained within the "elastic domain",which is defined by the coupling between two well-known limiting curves,Drucker and von Mises.

If the stress-point is beyond the limiting curve,the stress state is "illegal",and the point must be replaced on the limiting curve (which is assumed as plastic potential),adding into the element a set of permanent strains $\underline{\epsilon}^*$,i.e. the plastic strains $\delta\underline{\epsilon}_p$. The $\underline{\epsilon}^*$ tensor is determined on the basis of "orthogonality condition", respect to the plastic stress variation. Such determination of tensor $\underline{\epsilon}^*$ is performed,at first instance,on the element with fixed nodes; the stress tensor originated is:

$$\delta\underline{\sigma}=-\underline{\underline{K}}*\underline{\epsilon}^*$$

where $\underline{\underline{K}}$ is the "stiffness matrix" of masonry (here supposed isotropic),for plane-stress state. It must be verified that

$$\delta\underline{\sigma}=-\underline{\underline{K}}*\Gamma*\begin{vmatrix}\delta F/\delta\sigma_1\\ \delta F/\delta\sigma_2\end{vmatrix}$$

where the coefficient Γ is determined to allow the stress-point P to return on the limiting curve $F(\sigma_1\ \sigma_2)=0$.
$\delta\underline{\sigma}$ originates a set of fixed nodes unbalanced reactions;therefore, this phase is followed by a "relaxation" cycle consisting of their diffusion within the whole system.Each of these relaxational cycles generally produces a new incompatible state of stress. To obtain the elasto-plastic equilibrium several relaxational cycles are necessary within each loading step. Once the convergence has been achieved,the displacements of all the nodes,the stress state,the permanent strains stored and the energy dissipation in each element are obtained. It is also possible to reproduce a brittle type behaviour;the value ϵ_{max} of the maximum permanent strain is determined;we define a limiting value ϵ_o representing the maximum plastic strain,limit value for plasticity above brittle behaviour.If $\epsilon_{max}>\epsilon_o$,then the element cannot bear any stress state and its limiting curve degenerates to the origin of the stress plane $\sigma_1-\sigma_2$.Therefore the value of ϵ^* to be added must be defined to replace the stress-point into the origin.Such a cracked element cannot further contribute ot the energy dissipation process.
This poster deals with the strengthening of a masonry building in Potenza (Italy),(see illustration and photographs).The design criteria are the same applied in several other buildings the authors have restored in this country, were serious demages were suffered for the earthquake of Nov. 1980
The more significant details of the project are shown;the stress analysis of a masonry panel with opening,provided of pre-stressed steel cables,is illustrated.To evaluate the safety-factor in the panel,and to calibrate the design parameters,more than one analysis has been carried out.
For the shown example we have:
- average compression stress in masonry for gravity load: -0.19 N/mmq
- average compression stress in masonry due to pre-sterssing: -0,2 N/mmq
- shear forces distributed along panel's bounds: Γ*0,098 N/mmq
- width of the masonry wall: 500 mm

- total area of vertical pre-stressed reinforcements: 4*1.824 cmq
- masonry compressive strength: -2 N/mmq
- masonry tensile strength: +0.2 N/mmq
- limiting value for plasticity above brittle behavior: $\epsilon_o=5*10^{-4}$

It is illustrated the assumed "elastic domain" for masonry,and the "mesh" for the f.e.m.analysis,the shear-stress diagrams with,and without,prestressing.Some pictures have been taken from the computer-display,and they show plastic and cracked zones for more values of Γ.
The results of the analysis allow to state that enough safety is assured by the adopted values.The procedure avoids a vertification exclusively based on simple geometrical design rules,and introduces also for masonry more modern criteria about structural safety and reliability.

[1] Russo-Spena F., Sparacio R. = Verifica di un intervento di restauro statico con il metodo degli elementi finiti = Convegno ASSIRCO Palermo 1979.

Leere Seite
Blank page
Page vide